Economic Geology
Vol. 96, 2001, pp. 307–324

Geology of the Escondida Porphyry Copper Deposit, Antofagasta Region, Chile

Ruben A. Padilla Garza,[†]

BHP Minerals and Department of Geosciences, University of Arizona, Tucson, Arizona 85721

Spencer R. Titley,

Department of Geosciences, University of Arizona, Tucson, Arizona 85721

and Francisco Pimentel B.

Minera Escondida Limitada, avenida de la minera 501, Antofagasta, Chile

Abstract

The Escondida porphyry copper deposit, located in northern Chile, was one of the two largest copper producers of the world in the 1990s. The hydrothermal evolution of this deposit is associated with the emplacement of a late Eocene-Oligocene quartz monzonitic to granodioritic intrusive stock complex composed of at least three intrusive phases and hosted by Paleocene andesite. This Paleocene andesite is underlain by Mesozoic and Paleozoic sedimentary and volcanic rocks, which are characteristic of the basement of the Precordillera de Domeyko province in northern Chile. We propose that the intrusive stock associated with the mineralization at Escondida was emplaced in a tensional gash formed between sinistral strike-slip faults of the regional Domeyko fault system.

The complete evolution of the porphyry system is characterized by overprinting of pervasive and vein-associated alteration-mineralization styles grouped in three main hydrothermal stages. The early stage includes a zone of pervasive biotitization of andesite and development of a silicification shell around the intrusive complex, propylitic alteration around the biotitic zone, and a vein-associated orthoclase-quartz ± anhydrite-biotite alteration that mark the end of stage one. This early alteration contains magnetite, chalcopyrite, and bornite, with less than 0.5 vol percent of sulfides and a hypogene copper grade of ≤0.2 wt percent.

The second hydrothermal stage is represented by vein and vein selvage-associated chlorite-sericite ± quartz and by quartz-sericite with sulfides including chalcopyrite, pyrite, and molybdenite. In the chlorite-sericite and quartz-sericite zones the content of sulfides ranges from less than 0.5 to 2 vol percent with a chalcopyrite to pyrite ratio of 3 to 1 and copper grades that range between 0.4 and 0.6 wt percent. The intrusion of a rhyolite dike and a dome are at least 3 m.y. younger than the first and second hydrothermal stages and separate them in time from the late hydrothermal stage.

The late hydrothermal stage is represented by an acid-sulfate mineral association that includes pyrophyllite, alunite, and quartz as alteration minerals and a variety of sulfides that include bornite, chalcopyrite, pyrite, chalcocite, covellite, enargite, sphalerite, tennantite, and galena. This acid-sulfate event occurred mainly in west-northwest–striking veins and also along the contact of the rhyolite and its host rock. Where sulfides from this event overprint previous sulfides, the primary copper grades range from 0.6 to higher than 1.0 wt percent. In the Escondida deposit, the highest hypogene and supergene copper grades occur in areas where all three hydrothermal stages are present.

Introduction

This paper presents an update of the geology of the Escondida porphyry copper deposit in northern Chile (Fig. 1), which currently is one of the two largest copper producers in the world. The Escondida porphyry copper deposit, typical of many of its genetic class, is one of the largest in the world and in 1999 was producing more than 800,000 tons (t) of fine copper per year (http://www.bhp.com.au). In 1999 its reserves and resources in closely contiguous and related ore systems was 2,262 million tons (Mt) with 1.15 wt percent of copper (http://www.bhp.com.au). The deposit was discovered in 1981 and began production in 1989. The geology and history of its discovery and development has been outlined by Ortiz et al. (1996).

The deposit is one of several giants, including Chuquicamata, El Salvador, El Abra, and Collahuasi, located in northern Chile in and along the Domeyko Cordillera and the western limit of the Preandean Basin provinces (Fig. 1). This line of great ore deposits lies 100 km west of the high Andes. Escondida is similar in many respects to these other ore systems in being localized in porphyry intrusions that have invaded a volcanic pile. The basement is characteristic of the setting along this axis and consists of lower Paleozoic sedimentary rocks overlain by late Paleozoic-Early Triassic rhyolitic rocks, which in turn are overlain by a varied succession of Mesozoic clastic rocks with a few volcanic strata. Early Tertiary volcanic rocks, dominantly andesite, overlie the older successions and are hosts to the porphyry intrusions at Escondida.

Information from drill holes and surface exposures was used to develop the first geologic description and geochronology of alteration of the deposit (Alpers, 1986; Ojeda, 1986, 1990; Alpers and Brimhall, 1988, 1989). Since the publication of those works additional drill holes and mining have further exposed the orebody. This paper integrates the older information with new data to broaden the geologic knowledge of Escondida. New district mapping and regional geologic

[†] Corresponding author: e-mail, padilla.ruben.ra@bhp.com

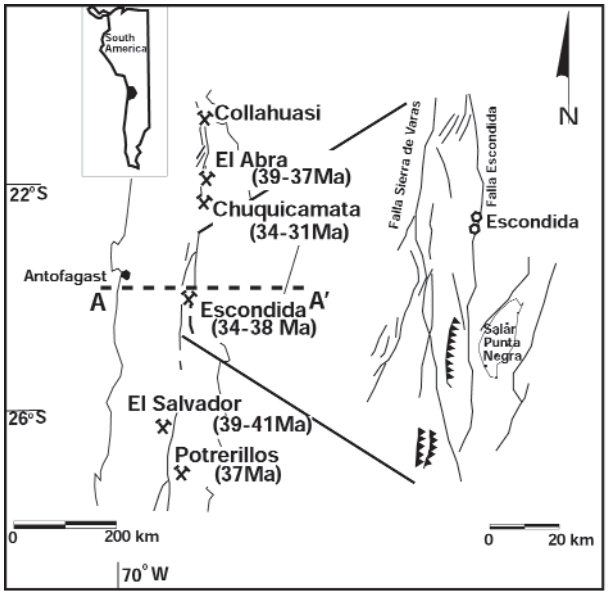

FIG. 1. Location of the Antofagasta region, the Domeyko fault system, and associated porphyry copper districts, the Escondida segment, and the Escondida district. After Mpodozis et al. (1993). Age of Escondida from Richards et al. (1999, 2001). See Figure 2 for section A-A'.

analysis of public data, in addition to new lithological, structural, alteration, and mineralization mapping of the deposit have provided further insights regarding the evolution of the deposit and its geologic setting.

Regional Geologic Setting

Five north-south morphotectonic-physiographic provinces characterize northern Chile (Sillitoe and McKee, 1996); from the Pacific coast eastward they are Coastal Range, Central Depression, Cordillera de Domeyko, Preandean Basin, and Andean Cordillera (Fig. 2). Escondida is located in the eastern limit of the Cordillera de Domeyko province (Fig. 2). The Cordillera de Domeyko province is approximately 50 km wide and is formed by north-south elongated ranges and shallow basins filled with gravel. Elevations vary from 2,000 to 4,500 m above sea level.

The earliest stage in the geologic evolution of this section of northern Chile is associated with the construction of the western margin of Gondwana during the Paleozoic (Ramos, 1988). In the province of the Preandean Basin and extending toward the east into Argentina and Bolivia, late Precambrian to middle Paleozoic turbidites and volcano-sedimentary sequences accumulated and were deformed when intra-arc basins opened and closed between Precambrian fragments that were located in front of the continent and were accreted during the middle Paleozoic (Ramos, 1988; Fig. 2). This early stage was followed by uplift and the development of a middle Paleozoic magmatic arc in the present position of the Precordillera de Domeyko and the Preandean Basin provinces (Mpodozis and Ramos, 1990; Fig. 2). A passive margin was formed from Middle Silurian to the late Carboniferous with rifting of the western margin of the continent (Bahlgurg and Herve, 1997). During this time a second sequence of turbidites accumulated along fluvial channels in the uplifted continental basement (Cordillera de Domeyko and Preandean Basin) and in deep extensional oceanic basins formed in the Coastal Range and in the Central Depression provinces (Bahlgurg and Herve, 1997; Fig. 2). Permian to Early Triassic rhyolitic rocks were emplaced in the western margin of the continent (Mpodozis and Ramos, 1990). By the end of the Paleozoic the western margin of this part of the Paleozoic continent and its oceanic edge were already formed, with a thick continental crust toward the east and turbidite basins, probably deposited on oceanic crust, toward the west. Today, the Cordillera de Domeyko is located at the boundary between these two zones (Fig. 2).

The Mesozoic was characterized by the development of a magmatic arc, in the Coastal Range province, and an extensional back-arc basin developed on the top of the Paleozoic basement of the Central Depression and on the Cordillera de Domeyko provinces (Sillitoe, 1981, 1988; Mpodozis and Ramos, 1990; Fig. 2). The last stage in the formation of this region was characterized by a continental margin where three Andean-type magmatic arcs evolved from Late Cretaceous through late Cenozoic, mainly in the eastern limit of the Central Depression, the Cordillera de Domeyko, and the Andean Cordillera provinces (Sillitoe, 1981, 1988; Mpodozis and Ramos, 1990; Fig. 2). The largest porphyry copper systems of the region were developed within the Precordillera de Domeyko and its western margin between 42 and 31 Ma (Gustafson and Hunt, 1975; Sillitoe, 1988; Zentilli et al., 1994; Cornejo and Mpodozis, 1996; Richards et al., 2001). From 31 Ma to the present, climatic changes favored the formation and preservation of enrichment blankets on the porphyry copper deposits (Alpers and Brimhall, 1988; Sillitoe and McKee, 1996).

Regional structure

The Domeyko fault system is the main structural feature of the Cordillera de Domeyko province. Mpodozis et al. (1993) separated the Domeyko fault system into five segments along its strike; each of these segments has characteristic local structural features that differentiate them from each other (Fig. 1). The Escondida district is located in the Escondida segment and is characterized by cymoid-shape (McKinstry, 1948), north-south elongated basins in a zone 200 km long by 20 to 50 km wide. During the Mesozoic the region of the Cordillera de Domeyko and the Central Depression were occupied by an extensional back-arc basin. The distribution of Paleozoic and Mesozoic rocks and the change of sedimentary facies of the rocks of the Mesozoic back-arc basin (Boric et al., 1990; Prinz et al., 1994; Ardill et al., 1998) suggest that the eastern limit of the Mesozoic extensional back-arc basin developed roughly in the transition between the Paleozoic continental crust and Paleozoic oceanic turbidites. Therefore, during the Mesozoic, the eastern edge of the back-arc basin was probably delimited by synsedimentary normal faults (Fig. 2). These types of growth faults have been reported in the area of Quebrada Blanca by Tomlinson and Blanco (1997a, b).

In the Cordillera de Domeyko, during the Late Cretaceous, the normal faults of this Mesozoic basin were probably inverted with the consequent formation of thrust faults, north-south folds, and crustal thickening. Reutter and Sheuber (1991) suggest a minimum of 25 percent of shortening for this

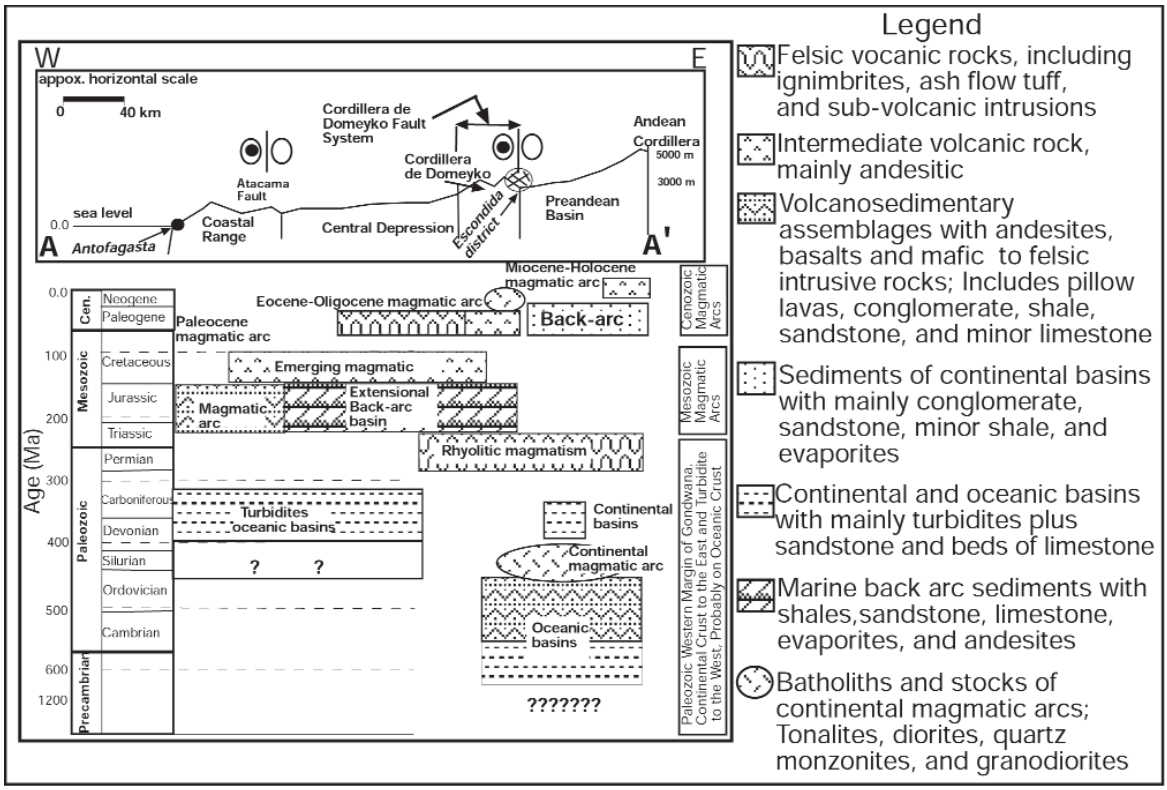

FIG. 2. At top, east-west section (A-A'), looking north from Antofagasta to Escondida, including the main morphotectonic provinces and the main fault systems of the region. At bottom, a generalized tectonostratigraphic column along the A-A' section. Compilations after Boric et al. (1990), Mpodozis and Ramos (1990), Mpodozis et al. (1993), Coney and Evenchick (1994), and Prinz et al. (1994).

period. From the Eocene to the Miocene, the structural deformation in the Cordillera de Domeyko province was characterized by transcurrent tectonics with a complex history of inversions of sense of movements (Mpodozis and Ramos, 1990; Reutter and Sheuber, 1991; Cornejo and Mpodozis, 1996; Tomlinson and Blanco, 1997a, b). During the early Eocene, the faults of the Domeyko fault system were active as transpressive structures as is indicated by the first reverse-strike-slip movements along the major faults (Cornejo and Mpodozis, 1996,Tomlinson and Blanco, 1997a, b). This transpressional tectonism continued active until 30 Ma, in the southern part of the region near El Salvador (Cornejo and Mpodozis, 1996). However, to the north, in the Chuquicamata district and in the central segment, near Escondida (Fig. 1), from 40 Ma to the present, the faults of the Domeyko fault system have moved as strike-slip structures (Mpodozis et al., 1993; Tomlinson and Blanco, 1997a, b). The only fault of the Domeyko system with reported significant lateral displacement is the West Fissure in Chiquicamata, where it truncates the copper deposit, with a proposed left lateral movement of 35 km (Baker and Guilbert, 1987; Dilles et al., 1997; Tomlinson and Blanco, 1997a, b).

Paleomagnetic reconstruction of plate movements from the Late lesozoic to the present indicates two main directions of subduction (Pardo-Casas and Molnar, 1987; Scheuber and Reutter, 1994). A northwest-southeast direction, older than 90 Ma, and a northeast-southwest direction younger than 70 Ma, with a transitional period between 90 and 70 Ma.

The Cretaceous sinistral sense of movement of the Atacama fault system, in the west coast of northern Chile, is in agreement with the northwest-southeast direction of convergence during this period. The Late Cretaceous compressional event that formed the majority of thrust faults and north-south folds in the Cordillera de Domeyko probably corresponds with the transitional period of rotation of stress direction, from northwest-southeast to northeast-southwest. Kinematic indicators of the Domeyko fault system reported by different authors (Boric et al., 1990; Mpodozis et al., 1993; Tomlinson and Blanco, 1997b; Veliz and Padilla, 1997) indicate different periods of rotation on the orientation of the main regional stress during the Paleocene-Miocene. The periods of sinistral sense of movement during the Cenozoic along the Domeyko system are in contradiction with the northeast-southwest direction of the main compressive stress suggested by the direction of subduction during this period. In spite of the northeast-southwest direction of subduction from 70 Ma to the present, the faults of the Domeyko fault system have sporadically moved in a left-lateral way, with calculated northwest-southeast orientation of the principal stress. This is an important problem in the evolution of the Domeyko fault system that has been addressed by Mpodozis et al. (1993) and by Tomlinson and Blanco (1997a); however, a detailed discussion of this problem is beyond the scope of this review.

Two of the largest porphyry copper districts of northern Chile are emplaced on faults of the Domeyko fault system.

North-northeast–striking faults have been associated with the emplacement of the porphyry copper system in Chuquicamata (Lindsay et al., 1995; Tomlinson and Blanco, 1997a), and a group of steeply dipping northwest-striking left-lateral faults are associated with the emplacement of the productive intrusive rocks in the Escondida district (see discussion below).

Summary and interpretation of the regional geologic setting

During the late Precambrian and the Paleozoic, this portion of northern Chile evolved as a part of the western margin of Gondwana (Ramos, 1988; Figs. 2 and 3), with a thick continental crust to the east and turbidite sediments toward the west, probably deposited on older oceanic crust. Today, the Cordillera de Domeyko is located at the boundary between these two zones (Fig. 2).

The Mesozoic marked an important change in the tectonic regime of the region. A new subduction zone was activated toward the west, forming a magmatic arc in the present position of the Coastal Range province, and its extensional back-arc basin developed over the area occupied today by the Central Depression and the Cordillera de Domeyko provinces (Mpodozis and Ramos, 1990; Figs. 2 and 3). During the Late Cretaceous and the entire Cenozoic, three Andean magmatic-arc types were developed cutting and covering previous rocks (Figs. 2 and 3). The mineralization at Escondida and many of the largest porphyry copper districts of northern Chile are spatially and temporarily associated with the Eocene-Oligocene magmatic event (Sillitoe, 1988; Cornejo and Mpodozis, 1996; Richards et al., 1999, 2001).

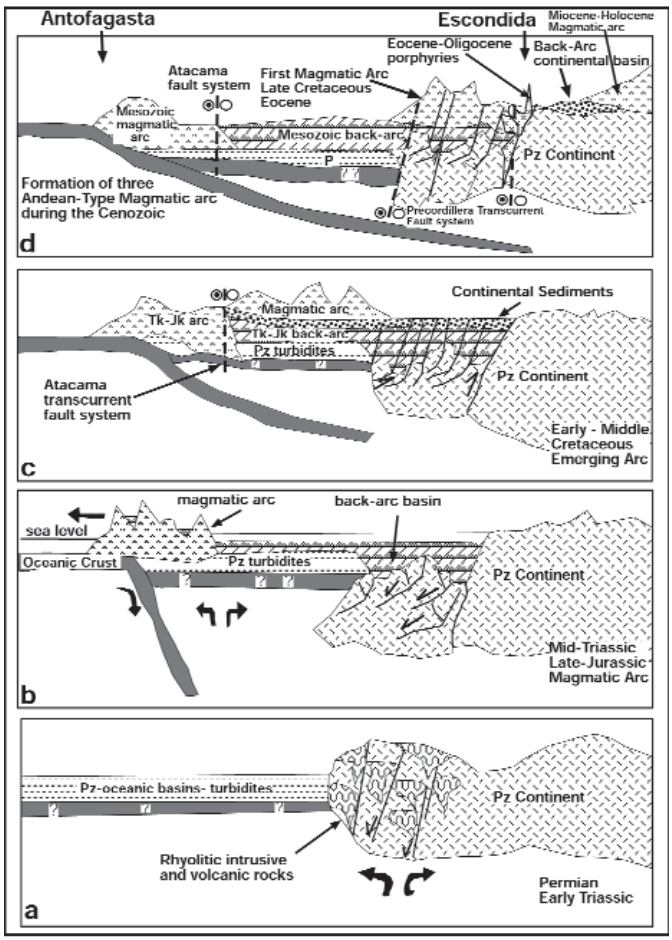

FIG. 3. Schematic section from Antofagasta to Escondida, presenting the interpreted geologic evolution of the region from Late Paleozoic to the Cenozoic.

The Cenozoic strike-slip structural deformation style of the Domeyko fault system followed periods of structural extension and shortening (Boric et al., 1990; Mpodozis and Ramos, 1990; Reutter and Sheuber, 1991; Cornejo and Mpodozis, 1996; Prinz et al., 1994; Tomlinson and Blanco, 1997a; Ardill et al., 1998). We conclude that the proto-Domeyko fault system could have developed during the formation of the Mesozoic extensional back-arc basin as growth faults that delimited the eastern edge of the extensional back-arc basin. It seems that this was not a continuous structure, but more likely, was formed by a series of north-south faults that broke the western margin of the Paleozoic continent in a 10- to 50-km-wide strip. Perhaps fragments of the Paleozoic continental crust were dropped down toward the west, to form the basement of the eastern edge of the Mesozoic back-arc basin (Fig. 3). It is possible that from the Late Cretaceous to the early Cenozoic, the set of faults formed during the Mesozoic were reactivated as thrust and transpressive faults that later moved as strike-slip structures forming the present geometry of the Domeyko fault system. It is suggested that the emplacement of productive magmas on the upper crust was favored by extensional zones along the strike-slip faults of the Domeyko fault system (see discussion of Escondida below). From 31 Ma to the present the region of the Cordillera de Domeyko has been tectonically quiet with low rates of denudation and climatic changes that favored the formation and preservation of enrichment blankets on the porphyry copper systems (Alpers and Brimhall, 1988; Sillitoe and McKee, 1996).

Geology of the Escondida District

The Escondida deposit is the largest of six different copper deposits located within the Escondida district. These deposits are Escondida Norte, Zaldivar, Pinta Verde, Carmen, Ricardo, and Escondida (Fig. 4). A simplified map of the geology of the Escondida district and distribution of ore deposits is presented in Figure 4. North-south–striking left-lateral strike-slip faults form a cymoidal shape that delimited the mineralized area in the district (Fig. 4). East of the central fault (the Zaldivar fault; Fig. 4), Paleozoic intrusive, volcanic, and sedimentary rocks correlated with the Argomedo and La Tabla Formations are exposed (Perelló, 1984; Marinovic et al., 1992; Richards et al., 2001). The base of this succession includes andesite with subordinate sedimentary lenses cut by tonalitic, granodioritic, and granitic intrusions. These units are cut and covered by Late Paleozoic rhyolitic rocks (Fig. 4). Paleozoic andesite is fine grained with trachytic texture, regionally affected by low-grade metamorphism characterized by epidote-chlorite ± tremolite, and contains up to 2 vol percent magnetite. The magnetism of this rock is a regional characteristic that makes the Paleozoic andesite easy to distinguish from Tertiary andesite, which is not magnetic. Whole-rock K-Ar analysis of the Paleozoic andesite in the Escondida district yielded apparent Jurassic ages of 196 ± 14

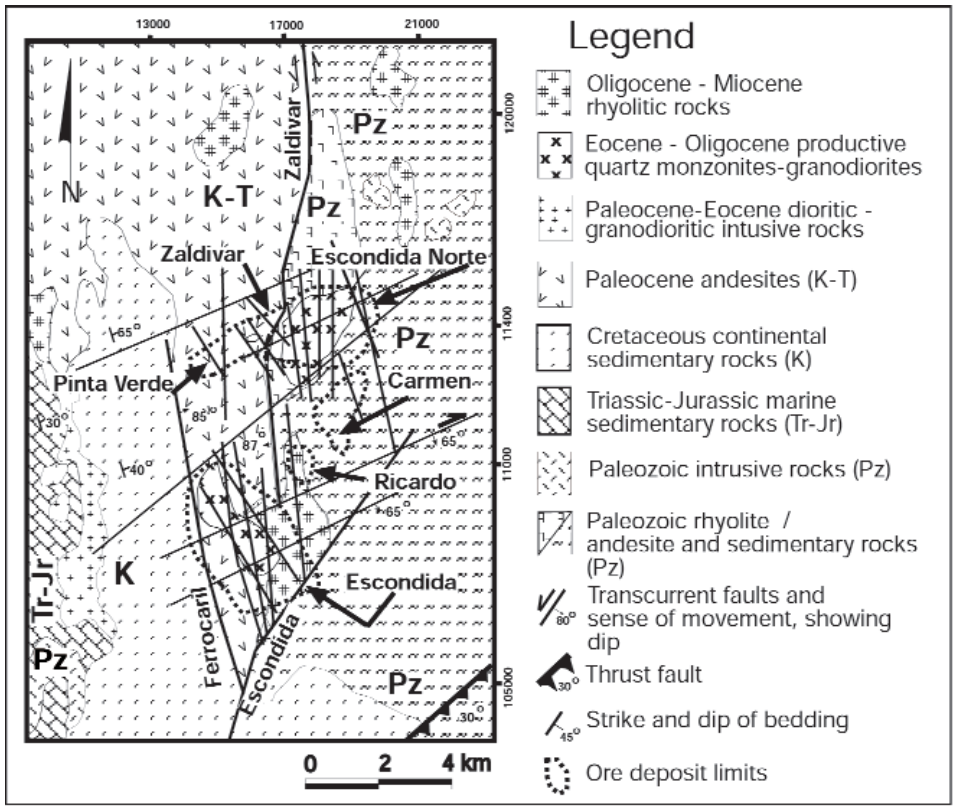

FIG. 4. Simplified geologic map of the Escondida district, showing locations of ore deposits. Compilation from outcrop mapping and drill hole information. After Perelló (1984), Marinovic et al. (1992), and this work. Map in UTM coordinates.

and 169 ± 12 Ma (Perelló, 1984; Marinovic et al., 1992). However, the trachytic andesite is clearly cut by a late Paleozoic rhyolite (268 ± 11 Ma, Marinovic et al., 1992; 265.8 ± 2.1 Ma, Richards et al., 2001) at the Escondida Norte deposit. Therefore, the whole-rock Jurassic ages of the andesite probably indicate the age of metamorphism. West of the Zaldivar fault (Fig. 4), Paleozoic rocks are overlain by marine and continental Mesozoic sedimentary rocks of the Profeta and Santa Ana Formations, respectively (Marinovic et al., 1992). The contact between the Paleozoic and Mesozoic units is exposed along the Antofagasta-Escondida highway. The contact is an unconformity marked by conglomerate and sandstone that change upward to shale, limestone, and calcareous limestone of the El Profeta Formation. The contact between the Triassic-Jurassic marine sediments and overlying middle Cretaceous continental-subaqueous rock is gradational. These middle Cretaceous rocks of the Santa Ana Formation consist principally of calcareous sandstone, red sandstone, conglomerate, and shale interbedded with thin layers of red volcanic tuffs. The Mesozoic sedimentary sequence is, in turn, overlain unconformably by Late Cretaceous-Paleocene andesite correlated with the Augusta Victoria Formation (Perelló, 1984; Fig. 4).

The Paleozoic-Mesozoic-Paleocene section is cut by Eocene-Oligocene (Richards et al., 2001) intrusive complexes, ranging from diorite to quartz monzonite and granodiorite. Some of these intrusive rocks may be associated with the copper mineralization in the Escondida district. Oligocene-Miocene rhyolitic subvolcanic intrusive and extrusive rocks cut and cover the Escondida porphyry (Alpers and Brimhall, 1988). Detailed timing relationships between the different intrusive rocks and the hydrothermal evolution in the district are still a subject of debate (cf. Richards et al., 2001).

The mineralization at Escondida, Zaldivar, and Escondida Norte is spatially and probably temporally related to the intrusion of quartz monzonitic and granodioritic stocks. In all three, alteration evolved from early potassic (that may have been synchronous with propylitic alteration), to sericite-chlorite, and quartz-sericite. These deposits also include the overprinting of a younger advanced argillic alteration event. Mineralization includes hypogene and supergene copper sulfides and copper oxides. At Escondida and Zaldivar, the intrusive rocks are hosted by Paleocene andesite, whereas at Escondida Norte they are hosted by the Paleozoic sequence (Fig. 4). At Pinta Verde the mineralization is hosted by Paleocene andesite with pervasive biotitic alteration with disseminated chalcopyrite, copper oxides, and sulfide veins. No porphyry phases have been found in direct association with this deposit. The Carmen deposit is covered by gravel, and there is not enough drilling information to describe its main characteristics. The Ricardo deposit consists of secondary chalcocite, rimming pyrite within rhyolites, emplaced along the Zaldivar fault, and no hypogene copper minerals have been observed in this deposit (Fig. 4).

Geology of the Escondida Deposit

Lithology

The Escondida porphyry copper deposit is associated with a quartz monzonitic-granodioritic-porphyritic stock hosted by andesite that has been correlated with the Paleocene Augusta Victoria Formation (Perelló, 1984; Marinovic et al., 1992). This intrusive stock, known as the Escondida stock, is composed of at least three phases (Perrello, 1983; Quiroz, 1998). Its shape is elliptical, elongated N 30° to 40°W with a 4.5-km-max axis and a 2.5-km-min axis (Fig. 5).

The earliest two intrusive phases are porphyritic rocks and are similar in mineralogy, but they are distinguished on the basis of their average content of phenocrysts, vein continuity, and intensity of alteration (Perelló, 1983; Quiroz, 1998). The first intrusive phase is known as the Colorado Grande intrusion, which is cut by the Escondida intrusion (Quiroz, 1998). Richards et al. (1999) report a U-Pb age on zircons of the Colorado Grande intrusion of 37.9 ±1.1 Ma. This is a discordia lower intercept date with an upper intercept indicating Paleozoic inheritance.

The Colorado Grande intrusion is a crowded porphyry with an average content of phenocrysts of 60 vol percent, whereas the Escondida intrusion has an average content of phenocrysts lower than 40 vol percent. In both intrusions the sizes of phenocrysts normally range between 1 and 5 mm and rarely up to 8 mm. Phenocrysts comprise quartz, orthoclase, plagioclase, and biotite. Quartz phenocrysts range between 2 and 8 vol percent; the crystals have a subrounded shape, with sizes between 0.5 and 3.0 mm, sometimes with undulose extinction. Plagioclase phenocrysts (60–70 vol %), of oligoclase to andesine composition, have lengths between 0.5 and 5 mm, are euhedral to subeuhedral, and show concentric compositional zoning. Orthoclase phenocrysts (20–30 vol %) between 0.5 and 3.0 mm in length are subeuhedral and show Carlsbad twining. Brown biotite books are euhedral with diameters between 0.5 and 1.5 mm and 1 to 3 vol percent. The groundmass is composed of crystals smaller than 0.5 mm, mainly plagioclase, orthoclase, quartz, and biotite.

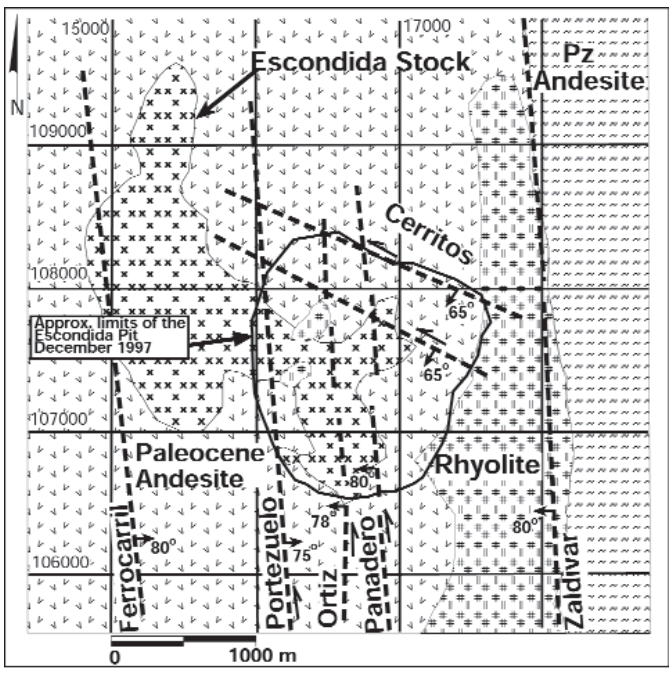

FIG. 5. Lithology and main fault zones of the Escondida deposit, plan view at 2,800 m above sea level. See Figures 6 and 7 for list of symbols. Compilation from drill hole information and mapping of the open pit. Approximate boundary of the Escondida open pit (1997) is shown. Map in local mine coordinates.

The third intrusive phase of the Escondida stock is the porphyry-breccia, which has a N 10° W elongated shape, with a maximum axis of 1 km and a minimum axis of 250 m (Fig. 6). This third intrusive phase is similar in composition and in content of phenocrysts to the Escondida intrusive phase but includes mineralized fragments of the two earlier intrusive phases and the andesite. The average content of fragments in this intrusive rock is approximately 8 vol percent; however, there are small volumes within it where fragments increase to 60 vol percent, showing the texture of an intrusive breccia. Mineralized veins also crosscut the porphyry-breccia intrusive phase. Quiroz (1998) recognized narrow granodioritic dikes with quartz-sericite alteration and hypogene Cu-Fe sulfides that cut all previous intrusive phases.

At least 3 m.y. after the emplacement of the Escondida stock and the development of the porphyry system, a rhyolitic dome and a rhyolitic dike were intruded and cut the Escondida porphyry stock (Alpers and Brimhall, 1988; Zentilli et al., 1994; Richards et al., 1999; Fig. 6). Zentilli et al. (1994) reported a U-Pb age on zircons of 32.6 ± 2 Ma from the rhyolitic dike of the west wall of the present pit. This is a discordia lower intercept date with an upper intercept indicating Paleozoic inheritance. Richards et al. (1999) suggested that if 2σ is used in the statistical calculation, the discordia lower intercept moves to 34.9 ± 0.4 Ma. Further statistical analysis of the available data and the generation of more data are warranted. The dome shape of this rhyolitic body is well preserved and can be observed in the present pit of Escondida.

The last intrusive event is marked by the intrusion of unmineralized, weakly sericite-altered, narrow quartz-monzonite dikes that cut the rhyolite (Fig. 6). Alpers and Brimhall (1988) reported K-Ar ages of sericite separated from these dikes of 31.5 ± 2.8 Ma and from whole-rock samples of these dikes of 31.0 ± 2.8 Ma.

In the evolution of the Escondida porphyry system at least four types of breccias were formed. Intrusive breccias are associated with the third intrusive phase of the Escondida stock; cooling breccias formed at the contact of the rhyolitic domes and the andesite; mineralized and barren pebble dikes that postdate the emplacement of the rhyolites; and tectonic breccias of different ages (Fig. 6).

Structure

Two main fault systems have been identified in the Escondida deposit: an early system formed by north-northwest–striking mineralized faults and a later system composed of northeast-striking postmineralization faults (Figs. 5, 7, and 8). The main strike of the regional Domeyko fault system coincides with the north-northwest direction of the mineralized fault system. Measurement of more than 1,800 structural features in the Escondida pit included azimuth and dip, crosscutting relationships, and timing with respect to miner-

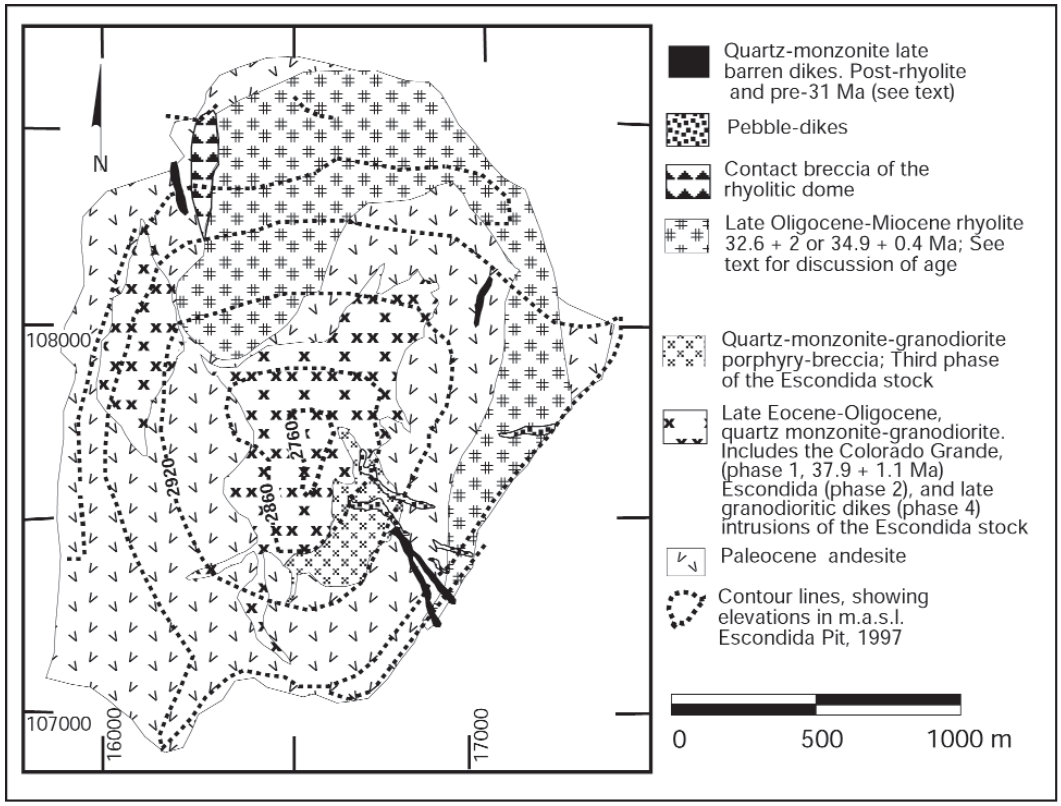

FIG. 6. Lithology of the Escondida pit. Ages of the Escondida stock and rhyolite from Richards et al. (1999, 2001) and from Zentilli et al. (1994).

alization. These data were used to define the geometric arrangement of faults presented in Figure 7. Of these structural data, 266 fault measurements include the trend and plunge of slickenlines observed on the fault surface and the displacement sense on the fault. These 266 data points were used to perform statistical analysis and to calculate the orientations of paleostress and paleostrain axes (Fig. 8). The sense of displacement on the fault planes was established using displacement sense criteria outlined by Pettit (1987) for brittle rocks.

Mineralized faults

Five north-northwest–striking mineralized fault zones are recognized at Escondida and include the Panadero, Ortiz, and Portezuelo zones within the open pit (Fig. 7); and the Zaldivar and Ferrocarril faults zones outside of the present pit (Fig. 5). The average strike of these mineralized fault zones is N 10° W, with variations between N 20° E and N 20° W. The main faults of the mineralized fault system located in the western part of the pit dip toward the east, whereas those in the eastern part of the pit dip toward the west, forming a grabenlike feature (Fig. 7). On benches above 2,700 m above sea level of the present pit, the N 10° W-striking fault zones are characterized by brittle cataclastic deformation, 50 to 250 m in width, with associated strongly altered N 10° W elongated areas that include north-northwest–striking veins with early quartz-sericitic and late advance argillic alteration (Fig. 6). The majority of late pebble dikes and late barren quartz-monzonitic dikes also present a north-northwest preferential orientation (Fig. 8). Individual fault planes within fault zones are identified by having continuous planes with a thickness up to 0.5 m of fractured rock or gouge. These individual planes present undulating surfaces along their strike and dip. The maximum continuity of individual fault planes parallel to the main strike is less than 1,000 m, but the continuity of the fault zones persist with parallel structures (Fig. 7). In some instances the limits of these main fault zones are clearly defined by sharp transitions from strongly broken and altered rock to a less altered rock. However, their limits are normally gradational and include a series of faults parallel to the main zone and a series of west-northwest–striking cross faults or stepover faults. The association of the main and the secondary west-northwest–striking structures form rhombic geometries within the fault zones. The less continuous west-northwest–striking faults are mineralized and strike between N 20° W and N 70° W. The dips of these faults shallow as they approach the main N 10° W-trending fault planes.

The principal N 10° W-striking faults exhibit continuities up to 1,000 m within the andesites, but their continuities decrease in the intrusive rocks. For example, faults of the Ortiz zone (Fig.7) are continuous in the andesites near the contact with the Escondida stock. However, within the central part of the stock the faults of this zone become discontinuous. At the eastern contact of the Escondida stock with the andesite, the Ortiz fault zone forms, in plan view, a rhombic-shape fracture zone approximately 700 m long and 200 m wide. The vertical geometry of this rhombic structure can be observed in the southeastern wall of the open pit where the fracture zone narrows down, so that the cross section of the fault zone

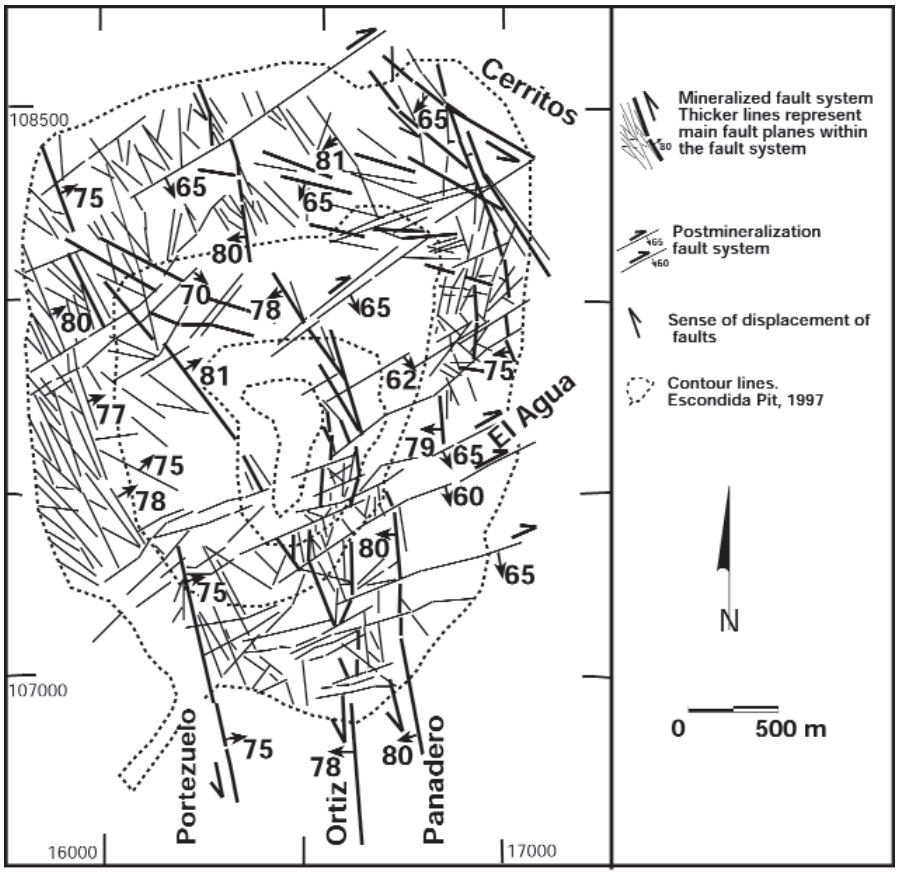

FIG. 7. Structures of the Escondida open pit. After Veliz and Padilla (1997).

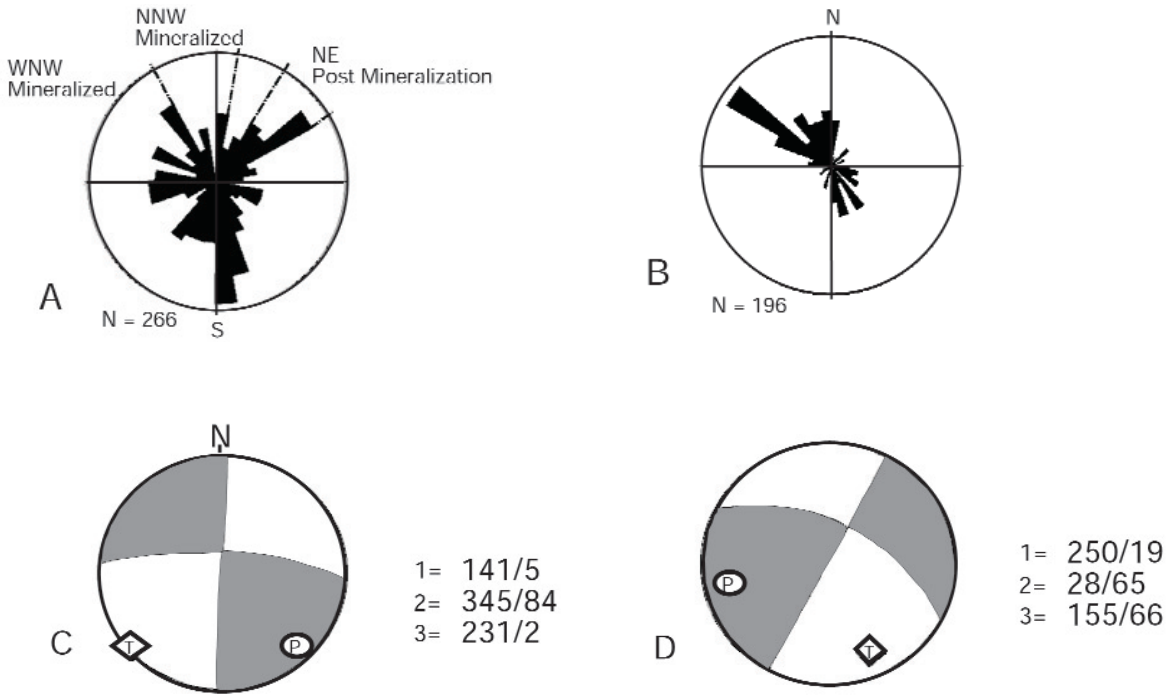

FIG. 8. Rose diagrams of structural data from the Escondida deposit using data from Figure 7. A. All fault systems. B. Quartz-sericite and advanced argillic mineralized veins, pebble dikes, and late barren dikes. P and T axes directions and paleostress orientations. C. Mineralized fault system. D. Postmineralization fault system. P-T axes were calculated with the software FAULKIN (Allmendinger et al., 1993). Paleostress orientations were calculated using the fault inversion software Brute 3 (Hardcastle and Hills, 1991).

displays a positive flower structure geometry (Woodcock and Schubert, 1994).

Postmineral faults

The second system of faults is represented by nonmineralized faults that postdate the emplacement of the intrusive rocks and the mineralization. This system exhibits a dextral sense of displacement along northeast-striking faults that dip between 60° and 70° S (Fig.7). This late fault system is characterized by a series of thin, 0.3-m-thick, continuous faults comprising a highly fractured zone with red clay gouge and sharp contacts. Some of these faults show lateral continuities greater than 2,000 m (Fig. 7), and they are the main pathways of water in the present open pit. Recognized displacements along these faults are less than 50 m in a dextral-lateral sense. At the regional scale, lineaments of this orientation are observed in satellite images even in areas covered by Miocene gravel.

Steeply dipping fault planes and shallowly plunging slickenlines suggest that both fault systems are associated with the dominantly transcurrent regional Domeyko fault system. Late, normal vertical reactivation along faults of both fault systems has displaced the enrichment blanket from 10 to 50 m.

Orientations of paleostress were calculated using the software Brute 3 (Hardcastle and Hills, 1991), a grid search method that calculates the best fit orientations for $\sigma 1$, $\sigma 2$, and $\sigma 3$. The program uses a datafile containing the strike and dip of each fault plane, the rake and plunge of slickenlines, and the relative sense of motion along each fault. Paleostrain calculations were completed using the software FOLKIN (Allmendinger et al., 1993) that uses a graphical method to calculate the infinitesimal principal shortening (P, Fig. 8C) and extension (T, Fig. 8C) axes, which may, but do not have to, coincide with the principal stress directions (Allmendinger et al., 1989). The calculated directions yield the estimated paleostress and paleostrain associated with the last movement of the mineralized and postmineralization fault systems and are shown in Figure 8. These data suggest a northwest-southeast axis of maximum compressive stress for mineralized faults, and an east-northeast–west-southwest principal compressive stress axis for the postmineralization faults.

Hydrothermal alteration

At Escondida, both time and space must serve as bases to understand the alteration process. Overprinting of both pervasive and vein-veinlet alteration by younger alteration types marks the style of evolution. The alteration process was dynamic, not static; consequently, rigorous definitions of zones and stages of alteration must incorporate the reality of sequential evolution. Stages are used in this paper to group alteration effects in time, and zoning is used to indicate the distribution in space of mineral associations. Sulfide assemblages also vary with each hydrothermal stage; however, they will be discussed in detail in the next section.

The study and description of deep hypogene hydrothermal features are complicated by the high-level, deeply penetrating effects of a late advanced argillic event and by subsequent supergene alteration that modified both the deep and shallow hydrothermal features. Different alteration mineral assemblages are not necessarily exclusive to recognized zones of alteration. Figure 9 shows the distribution of alteration zones.

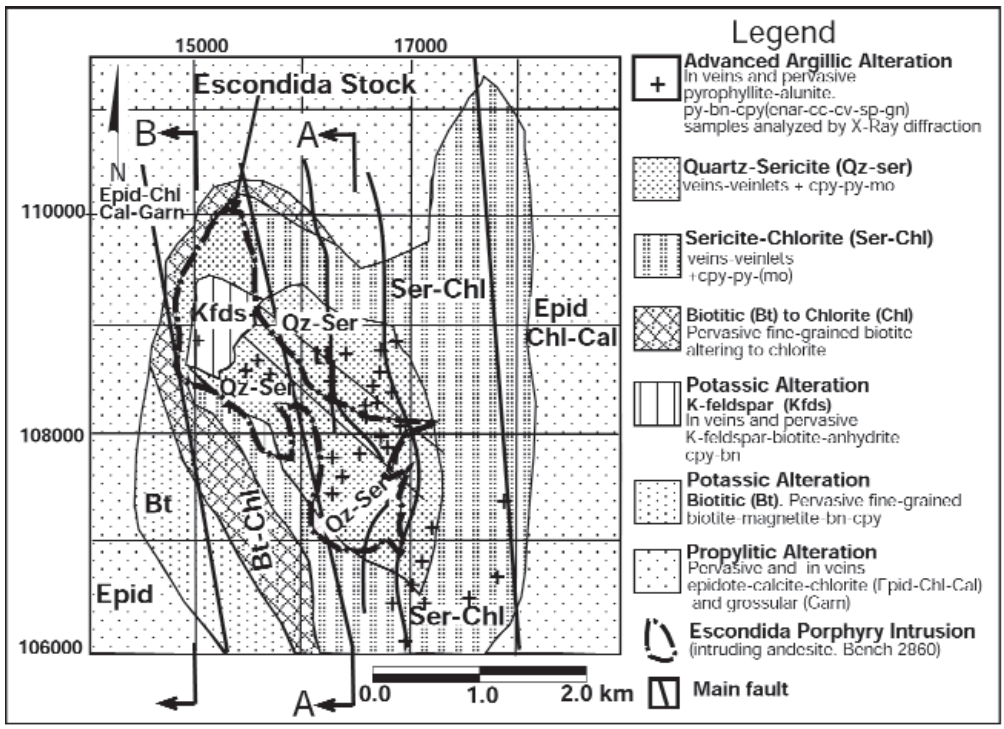

FIG. 9. Plan view showing dominant hypogene alteration mineral associations. From 100 to 650 m below surface. Compilation from drill hole information and the geology of the open pit. Abbreviations: bn = bornite, bt = biotite, cal = calcite, chl = chlorite, cpy = chalcopyrite, enar = enargite, epid = epidote, garn = grossular, gn = galena, Kfds = orthoclase, mag = magnetite, mo = molybdenite, py = pyrite, qz = quartz, ser = sericite, sp = sphalerite

Despite the dynamic evolving characteristics of the system, three main stages of alteration, here designated stages 1, 2, and 3, can be defined based on mineral associations and their mode of occurrence in space and time (Table 1).

The effects of the early or stage 1 processes are seen in both pervasive alteration styles and in alteration of some stockwork veins and veinlets. Two pervasive alteration types are present in stage 1. These were synchronous and are interpreted as manifestations of the earliest stages of intrusive igneous activity. The mafic phenocrysts and the groundmass of the andesite wall rock of the porphyry complex have been extensively and locally completely altered to biotite. Although affected by later hypogene alteration, weathered and modified by acid supergene effects, these biotite-altered rocks

TABLE 1. Characteristics of the Three Main Hydrothermal Stages at the Escondida Porphyry Copper Deposit

	Mineral assemblages	Main characteristics of veins	Comments
Stage 1 ~38 Ma	Propylitic Pervasive and vein-veinlet alteration including epidote-chlorite-zeolites ± pyrite and rarely chalcopyrite, grossular, and albite; probably started during stage 1 and evolved during the development of stages 2 and 3 Silicification Pervasive fine-grained silicification shell at the contact intrusive rock-andesite host rock. Interpreted as contact effect during the emplacement of the Escondia stock Potassic Pervasive fine-grained biotite with minor orthoclase affecting the andesitic host rock; magnetite- bornite-chalcopyrite Pervasive but mainly in veins controlled orthoclase +quartz ± biotite-anhydrite; with bornite-chalcopyrite; mainly affecting the Escondida stock	Veins of stage 1 represent the transition between early pervasive and later vein-veinlet alteration styles Veins 1a Sinuous and discontinuous barren quartz veins Veins 1b Irregular but more continuous than 1a veins; center and halo formed by orthoclase + quartz ± biotite-anhydrite; with bornite-chalcopyrite Veins 1c Quartz veins with no alteration halo; more continuos veins than 1a and 1b; with chalcopyrite and bornite	Total content of sulfides with the potassic assemblages <0.5 vol %, with hypogene copper grades ≤0.2 wt %; veins 1a and 1b are similar to A veins described at the El Salvador, whereas 1c veins are similar to B veins from the El Salvador deposit; however, no molybdenite has been observed with these veins at Escondida
Stage 2 ~38 Ma	Chlorite-sericite ± quartz Vein-controlled alteration, affecting biotitic-altered andesite; in the intrusive rock, chlorite selectively altered mafic minerals and sometimes orthoclase; within the intrusive rock, chlorite also occurs in <1-mm cracks that cut veins from stage 1; chalcopyrite ± pyrite-molybdenite Quartz -sericite (greenish-grayish) Vein-controlled alteration mainly within the intrusive rock and stronger along fault zones; sericite in halos presents pale green to gray colors; associated sulfides are chalcopyrite ± pyrite-molybdenite Pyrite-sericite (white) Vein-controlled alteration formed of pyrite ± chalcopyrite and strong halos of white sericite and disseminated pyrite	Veins 2a Associated with the chlorite sericite assemblage there are thin sulfide veins (<5 mm) with none or minor amounts of quartz; alteration halos are of sericite-chlorite with sulfides, that grade outward to dominantly chlorite, replacing biotite in the biotitic-altered andesite; sulfides include chalcopyrite ± pyrite-mobybdenite Veins 2b With the sericite-quartz assemblage veins are formed by quartz sulfide with thick quartz-sericite (pale green and gray) halos; associated sulfides are chalcopyrite ± pyrite-mobybdenite Veins 2c Associated with the last sericitic event there are pyrite ± chalcopyrite veins with white sericite-pyrite halos	Veins of stage 2 are irregular and less sinuous than the veins of stage 1; very often veins of stage 2 reopened veins of stage 1; bornite and magnetite are no longer present in this stage, whereas molybdenite and pyrite appear for the first time in the porphyry system; sulfide content increases to 2 vol % with chlorite-sericite and quartz-sericite (greenish-grayish sericite), with a pyrite/chalcopyrite of 1/3; with the white sericite-pyrite event total content of sulfides can go locally to 5 vol % with a pyrite/chalcopyrite up to 10/1; where this stage is strong, Cu grades vary between 0.4 and 0.6 wt %; vein types similar to 2b and 2c were classified as D veins at the El Salvador deposit
Stage 3 ≤38 Ma	Advanced argillic Pyrophyllite-sericite-quartz-alunite with abundant sulfides including bornite-chalcopyrite, pyrite, lamellar covellite, minor amounts of chalcocite, enargite, sphalerite with exsolutions of tennantite and chalcopyrite, and galena; pervasive at the contact of rhyolite with its host rock, but its main occurrence is in N 40° W veins within major fault zones	Veins 3 Continuous veins, up to 2 m wide; banded internal textures starting with quartz, followed by bornite-chalcopyrite, pyrite-chalcopyrite, chalcopyrite-covellite-chalcocite, enargite, pyrite, sphalerite-chalcopyrie-tennantite, galena, and alunite	This is the only stage that affects the rhyolite; veins normally do not include the whole paragenetic sequence of sulfides; more often, veins include only pyrite with minor amounts of enargite, covellite, and alunite; similar veins were classified as D veins at the El Salvador deposit

were still conspicuous in pit benches in 1998. At the intrusion-volcanic rock contact, a second kind of pervasive alteration has taken place and is manifested by texturally destructive silicification, which has affected both rock types. Another type of pervasive alteration is represented by replacement of orthoclase in the groundmass of the Escondida intrusive stock. Drill hole data beneath supergene alteration indicate that local volumes, on the order of cubic meters, of the intrusive rock have been pervasively altered to orthoclase; although, much of the orthoclase alteration is seen in proximity to stockwork veins. The transition between pervasive and vein-controlled alteration is marked in the rocks of the mineralized center of the deposit by discontinuous veins of quartz and quartz-orthoclase.

Propylitic alteration as defined at Escondida is characterized by sporadic conversion of plagioclase to grossular and, more commonly, to epidote and montmorillonite by conversion of hornblende and biotite to chlorite and widespread carbonate and zeolite veins. The conversion of plagioclase to grossular was probably synchronous with development of biotite alteration in the andesite and orthoclase in the intrusive rock. Propylitic alteration surrounds the center of mineralization and its attendant early potassic alteration.

The early or stage 1 alteration was followed by the formation of alteration in selvages adjacent to stockwork veinlets. This alteration is separated into two successive mineral associations, chlorite-sericite ± quartz and quartz-sericite. The advanced argillic assemblage represents the latest alteration stage. Development of the advanced argillic alteration took place late in the life of the system when high-level fracture permeability had developed and progressed through the time of fracture formation, as indicated by the presence of quartz-enargite-pyrite-alunite veins in high-level pervasive assemblage.

Ojeda (1986) and Alpers and Brimhall (1988) reported a group of K-Ar ages of hydrothermal biotite and sericite, ranging between 33.7 ± 1.4 and 31.0 ± 1.4 Ma, with two other samples, ranging between 38.3 ± 3.0 and 39.1 ± 2.2 Ma. Therefore, the authors suggested that the hydrothermal evolution at Escondida took place between 33.7 ± 1.4 and 31.0 ± 1.4 Ma, dismissing the two older ages by arguing possible contamination and disagreement with the rest of the data. However, Richards et al. (2001) propose a 37.9 ±1.1 Ma age for the hydrothermal system at Escondida, coeval with the emplacement of the Colorado Grande intrusion. Richards et al. (2001) also suggest that the K-Ar ages reported by Alpers and Brimhall (1988) and Ojeda (1986) may represent the time of emplacement of the rhyolite that reset the original K-Ar system.

The temporal evolution of alteration reported here as stages is best documented by the overprinting of mineral associations and by crosscutting relationships of veins. The intensity of fracturing notations of this study follow from the work of Titley and Heidrick (1978): weak intensity, 0.2 cm^{-1}; moderate, 0.5 cm^{-1}; and intense, >1.0 cm^{-1}. In the following description of alteration, the terms intense, moderate, and weak alteration are used for the megascopic description of rocks. Intense alteration refers to rocks with their original mineral texture completely obliterated by alteration; exceptions include primary quartz grains unaffected by hydrothermal alteration of any type and relic plagioclase grains in andesite altered to the biotitic assemblage. Moderate alteration is a term for rocks, where in spite of almost complete hydrothermal alteration of individual mineral grains, the main textural characteristics of the rock can still be recognized. The term weak alteration describes rocks with mainly fresh characteristics but also with patches where alteration effects are recognizable under the hand lens.

Stage 1—potassic: Potassic alteration shows lithological control. In the Escondida stock, the early potassic alteration is represented mainly by weak disseminated K feldspar that replaces plagioclase crystals and groundmass of the intrusive rock, giving a pink tint to the rock. In andesite, it is characterized by secondary biotite with minor amounts of disseminated and vein-controlled K feldspar and anhydrite (Fig. 9, Table 1). The area of biotitic-altered andesite is semielliptical and changes outward to propylitic alteration and inward either to K feldspar-altered intrusive rock or chlorite-sericite in the same andesite (Fig. 9). Most of the biotite is fine grained (<0.1-mm diam) and replaces minerals in the groundmass of the rock and the mafic and plagioclase phenocrysts; however, the largest plagioclase phenocrysts are only partially affected by this alteration. In hand specimens, andesite with this type of alteration has a characteristic black color and the preservation of plagioclase ghosts now altered to montmorillonite reveal the original texture of the rock.

Stage 1—propylitic: Propylitic alteration is defined here by the development of assemblages containing epidote with minor amounts of chlorite, montmorillonite, minor biotite, and grossular, and widespread carbonate and zeolite veins (Fig. 9, Table 1). These alteration minerals replace amphibole and plagioclase in andesite. Grossular is found only replacing plagioclase. Some plagioclase crystals reveal an albitic halo. This propylitic alteration forms a halo around the potassic zone and is mainly pervasive with occasional partial or total destruction of the original mineral composition and texture of the andesite.

Stage 1—silicification shell: A shell of silicified rock is present at the contact between the andesite and the Escondida stock and is interpreted to represent a contact metasomatic phenomena. This silicification event has a width that varies between 20 and 40 m and affects both the andesite and the Escondida intrusion. The silicified rock is aphanitic, hard, and strongly fractured. In thin section the rock consists of an aggregate of fine-grained quartz with grain sizes smaller than 50 μm. This silicification zone is one of the earliest alteration events and is cut by veins associated with all alteration assemblages described below. This zone has been recognized in the present pit, but the degree of continuity along the stock contact has not yet been revealed.

Stage 1—early veins: The earliest veins contain quartz or quartz-orthoclase ± biotite ± anhydrite. The best samples of veins from the early stage were found in the northwestern part of the deposit as well as in the deepest zones sampled by drill holes. Moreover, relicts of those veins are found throughout the deposit, normally reopened by vein minerals deposited during later events. Veins of the early stage are subdivided into three subgroups: Stage 1a: strongly sinuous-curved and discontinuous quartz veins without alteration halos that occur mainly in the intrusive rock but also in andesite located near the contact with the intrusive rock; they

are generally no longer than 10 cm; their limits within the host rock are irregular but well defined, with widths that vary between 1 mm and 2 cm. Stage 1b: veins formed of quartz-K feldspar plus minor amounts of biotite and anhydrite; such veins are more continuous and less sinuous than type 1a; they are characterized by pink K feldspar alteration halo selvages that make the vein margins very irregular and poorly defined; the vein widths vary between 1 mm and 3 cm. Stage1c: continuous quartz veins without alteration halos that occur mainly within the intrusive rock; the walls of these veins are irregular but well defined, with lengths up to 70 cm and widths from less than 1 to 5 cm. This group of early veins shows multiple events of emplacement; however, type 1b and 1c veins postdate type 1a veins in most instances.

Stage 2—chlorite-sericite ± quartz: This alteration varies from dominantly chlorite to dominantly sericite. Disseminated and vein-controlled chlorite-sericite alteration affects the andesite with biotitic alteration. This alteration in the Escondida stock is represented by selective alteration of biotite and other mafic minerals, by the alteration of K feldspar of the potassic assemblage to chlorite-sericite, and by the introduction and precipitation of smaller amounts of chlorite in cracks of reopened veins. The original textures of the andesite and the intrusive rock are preserved, except in the center of the veins or in the first few centimeters of their alteration halos. Toward the outer limit of the chlorite-sericite zone—mainly in andesite—chlorite is more abundant than sericite, but sericite is more abundant in the rocks closer to the stock (Fig. 9). The width of this zone varies from 1 to 2 km and it is open on both the northeastern and the southeastern limits of the deposit (Fig. 9). In hand specimens, chlorite-sericite alteration is characterized by its dark to pastel green color. The density of fractures in this zone is moderate, with the formation of new veins preferentially within the andesite. Veins associated with the chlorite-sericite alteration of stage 2 are named here as type 2a veins. These veins cut or reopened the early veins described above. They have lengths that vary from a few centimeters up to 50 cm and they are normally thin, with thicknesses ranging from less than 1 to 3 cm. The type 2a veins of chlorite-sericite assemblage are more continuous than the veins associated with the potassic alteration, but their margins with the host rock are still irregular and diffuse. They are also sinuous and show branching geometries. In andesite, type 2a veins show zoning that starts with a <1-cm-wide vein filling formed by sulfides and normally without quartz or with minor amounts of quartz grains smaller than 50 μm. Outward, the alteration halo consists of a mixture of sericite and subordinate chlorite that changes outward to mainly dark green chlorite with subordinate sericite.

Stage 2—quartz-sericite: The quartz-sericite assemblage is the main alteration in the center of the deposit and affected the southeastern portion of the Escondida stock and the andesite close to the contact with the intrusive rock (Fig. 9). This mineral association occurs mainly in veins and in their alteration halos. When this alteration is very intense the rock is converted to a white textureless mass in which the intrusive rock can be distinguished only by the preserved quartz phenocrysts. The density of veins in this zone is intense. Veins associated with quartz-sericite alteration are named type 2b and 2c. They are usually longer than 20 cm and in some cases longer than 1 m, with thicknesses that vary from less than 1 up to 15 cm, and with irregular outer limits that grade from intense to moderate and weak quartz-sericitic alteration. In hand specimens this alteration is characterized by a mix of colors including pastel green, dark gray, and white. In such veins, the vein fillings consist of quartz and sulfides with alteration selvages formed by texturally destructive sericitic alteration. Outward, similar alteration continues but is less intense where the shapes of plagioclase and orthoclase phenocrysts are preserved. In this outer alteration zone of the veins, the tabular feldspar crystals are altered to sericite and they are surrounded by a pale green sericite in the groundmass. Microprobe analysis

of these pale green-gray alteration halos, with crystals sizes smaller than 50 μm, indicate that they are composed of aggregates of sericite and quartz.

Stage 3—advanced argillic: The latest hydrothermal stage of alteration in the Escondida deposit is represented by the acid-sulfate alteration that affected the andesite and the Escondida intrusion. This is also the only hypogene alteration that cuts the rhyolite. The distribution of this alteration is controlled by the main fault zones and by the contact between the rhyolite and the country rock. The spatial distribution of the advanced argillic alteration has been defined by locating more than 200 composite samples that were analyzed by X-ray diffraction (Alpers and Brimhall, 1988; Figs. 9 and 10). The mineralogical association that defines this alteration includes pervasive alteration to pyrophyllite, alunite, and quartz,

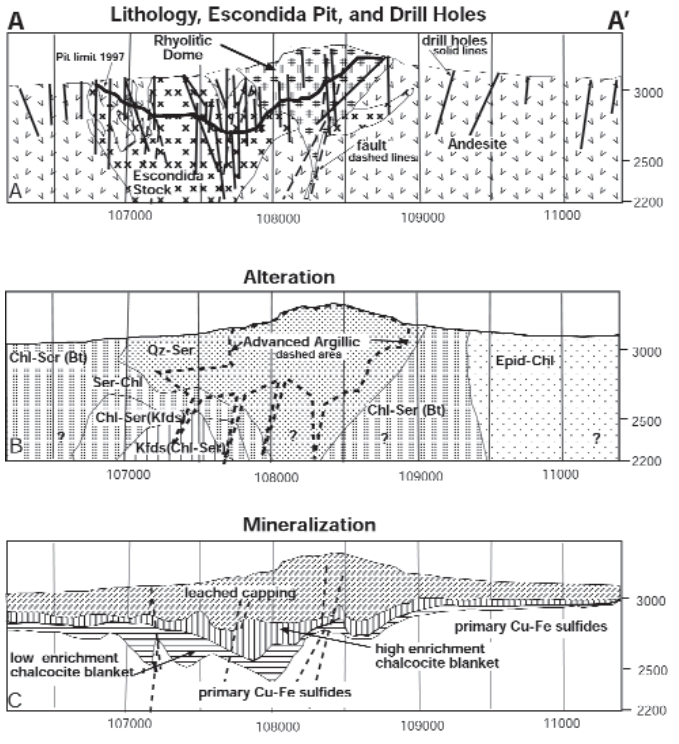

FIG. 10. Section N-S 16450, looking west. See Figures 5, 6, and 9 for locations and symbols. Dominant mineral alteration outside parenthesis and subordinated mineral alteration in parenthesis. High and low enrichment are subdivisions of the chalcocite blanket. High enrichment zone does no contain pyrite. Low enrichment zone contains few percentage of pyrite coexisting with the supergene copper sulfides.

presence of banded quartz veins, and abundant sulfides. In the contact between the rhyolitic dome or dike with the andesite this alteration is pervasive and has a characteristic mottled texture as a result of white pyrophyllite-sericite spots.

Veins of stage 3 show thicknesses that vary from a few millimeters up to 1 or 2 m with banded, massive, and breccia texture. These veins include at least two different types of euhedral quartz and abundant sulfides with minor amounts of alunite. Locally, the infilling of these veins is brecciated and cemented with alunite. At the margins of these veins, bands of fine-grained sugary quartz (up to 500-μm diam) and semitranslucent fine-grained quartz (<70-μm diam) have thicknesses between <1 and 10 cm.

Mineralization

Ore minerals in the Escondida deposit are grouped into three main ore types. These types include hypogene sulfides, supergene sulfides, and copper oxides. The discussion of the distribution of ore in this section was carried out on a copper resource that used a cutoff of 0.3 wt percent, which may result in a different tonnage and copper grade than the ore resources cited above. Out of this copper resource, 49 wt percent of the total tonnage is hosted by the Esocondia stock. In this intrusive rock the average copper grade, at this cutoff, is 1.12 wt percent and represents 59 wt percent of the total fine copper resource. The other 51 wt percent of the total tonnage is hosted by the andesite, which has an average copper grade of 0.75 wt percent and constitutes 41 wt percent of the total fine copper resource at a 0.3 cut off (Table 2).

Hypogene ore

The hypogene mineralization represents 30 percent of the presently calculated and discovered total copper resource at Escondida and is mainly present in the deepest parts of the deposit or at its margins; some also occurs as relict volumes within the supergene blanket (Figs. 10, 11). The three main hydrothermal stages described above also contain different Cu-Fe mineral associations (Table 1). During the early stage, magnetite-bornite-chalcopyrite ore is associated with biotite and K feldspar-quartz alteration, with a content of sulfides lower than 0.5 vol percent. At microscopic scale, it is common to observe veins of stage 1 reopened or crosscut by younger stages. Within stage 2 veins, chalcopyrite with minor amounts of molybdenite and pyrite are intergrown with sericite or chlorite-sericite. With this second mineralizing stage the content of sulfides increases up to 2 vol percent. The latest hydrothermal stage, represented by the acid-sulfate alteration, includes the largest variety of sulfides in the deposits, including chalcopyrite, bornite, pyrite, lamellar covellite and chalcocite, enargite, sphalerite, galena, and tennantite. These late assemblages formed new veins and also reopened older veins. This overprinting of hydrothermal events is reflected in the copper grade. Copper grades in areas of potassic alteration with weak overprinting by younger events are normally lower than 0.3 wt percent. In areas with strong quartz-sericitic alteration copper grades vary between 0.4 and 0.6 wt percent. Locally, where veins of sulfides from the last stage cut previous mineralization, the hypogene copper grades increase up to 1 wt percent or higher.

Within the propylitic alteration zone, pyrite is the most common sulfide, but there are local small volumes of pyrite-chalcopyrite in the veins. Copper grades are normally lower than 0.1 wt percent. In the potassic alteration zone, sulfide minerals are mainly chalcopyrite and bornite; however, the volume percentage of Cu-Fe sulfides and Fe oxides minerals varies depending on the dominant alteration mineral assemblage of the potassic alteration. For instance, andesite with pervasive biotite alteration contains up to 2 vol percent magnetite

TABLE 2. Total Mineralization by Rock Type, Escondida Deposit

Rock type	Proportion of rock in orebody (wt %)	Cu grade (wt %)	Proportion of total Cu (wt %)
Porphyry	49	1.12	59
Andesite	51	0.75	41
Total	100	0.9	100

Total mineralization by rock and ore type, Escondida deposit

	Rock type					
	Andesite			Porphyry		
Ore type	Proportion of ore type in orebody (wt %)	Cu grade by ore type (wt %)	Proportion of total Cu by ore type (wt %)	Proportion of ore type in orebody (wt %)	Cu grade by ore type (wt %)	Proportion of total Cu by ore type (wt %)
High enrichment	25	1.06	39	29	1.39	44
Low enrichment	17	0.69	18	27	0.96	28
Primary	42	0.54	34	34	0.66	25
Cu oxides (mixed)	16	0.57/0.35	9	10	0.59/0.37	3
Total	100	(Cu_t/Cu_s)	100	100	(Cu_t/Cu_s)	100

Notes: Cu_t = total copper grade, Cu_s = soluble copper grade; resources for these tables were calculated using a cutoff of 0.3 wt percent copper in the drill hole data base of Escondida; in 1999 announced ore reserves was 2,262 Mt with 1.15 wt percent copper

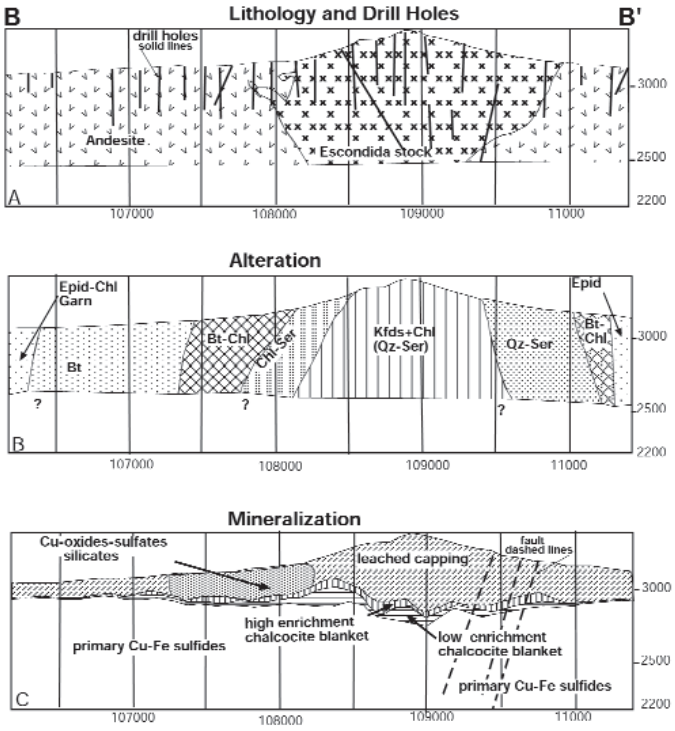

FIG. 11. Section N-S 15100, looking west. See Figures 5, 6, and 9 for locations and symbols. Dominant mineral alteration outside parenthesis and subordinated mineral alteration in parenthesis. High and low enrichment are subdivisions of the chalcocite blanket. High enrichment zone does no contain pyrite. Low enrichment zone contains a few percentage of pyrite coexisting with the supergene copper sulfides.

grains. Individual crystals of magnetite are smaller than 60 μm and sometimes are replaced by bornite and chalcopyrite. The total sulfide content of biotite-altered andesite is lower than 0.5 vol percent, and the copper grade is lower than 0.2 wt percent. The content of magnetite decreases with an increased presence of K feldspar-bearing veins. Within the intrusive rock or in the andesitic host rock, where the predominant potassic alteration assemblage is K feldspar-quartz ± biotite ± anhydrite the sulfides constitute less than 0.5 vol percent, and these include 90 vol percent chalcopyrite and <10 vol percent bornite, with grain sizes ranging between 20 to 600 μm in diameter. Bornite grains are normally smaller than 100 μm in diameter. Copper grades within volumes of rock mainly affected by K feldspar-quartz alteration vary from <0.1 to 0.3 wt percent (Table 1).

Within the volume of rock affected by chlorite-sericite ± quartz and quartz-sericite veins, of the second hydrothermal stage, the average total sulfide content increases up to 2 vol percent. The dominant sulfide is chalcopyrite with minor amounts of pyrite and molybdenite. The chalcopyrite to pyrite ratio is around 3:1. Where this second hydrothermal stage is strong the hypogene copper grades vary between 0.4 and 0.6 wt percent. Chlorite-sericite ± quartz veins in andesite contain up to 20 vol percent of sulfides within the thin vein and less than 2 vol percent in the alteration halo. The vein contains grains of sulfides between 50 and 500 μm in diameter; however, in the alteration halos the sulfide crystals are normally smaller than 30 μm in diameter. Within the Escondida stock, in quartz of the quartz-sericitic veins, sulfides occur in cracks with thicknesses <20 μm, between grain margins, or as disseminated sulfide grains up to 900 μm in diameter within quartz crystals. The content of sulfides increases up to 10 vol percent within the pale green intense alteration halos of the quartz-sericite alteration, with sulfide grains that vary between 50 and 600 μm in diameter. Outward, beyond the area of the intense alteration halos, where the porphyritic texture of the host rock is preserved, the sulfides decrease to less than 2 vol percent of the rock and are between 30 and 100 μm in diameter. Late quartz-sericite veins with dominantly white sericite and pyrite occur mainly in the center of the deposit along the main fault zones. With the presence of these veins the total content of sulfides increases up to 5 vol percent, and the hypogene copper grade is not affected. The vein filling of these pyrite-white sericite veins with quartz-sericitic halos is commonly formed by subeuhedral to euhedral pyrite crystals with diameters up to 3 mm.

The youngest hypogene sulfides were deposited during the acid-sulfate event that represents the third and latest hydrothermal stage. Veins of the acid-sulfate event are sulfide rich with banded textures that in some cases include the complete paragenetic evolution of this stage. Early in the evolution of the acid-sulfate veins, bornite-chalcopyrite and euhedral quartz precipitated. Later, these veins were reopened and pyrite precipitated and replaced the earlier bornite-chalcopyrite. After the pyritic event, these late veins were reopened and fragments of the earlier sulfides were cemented by chalcopyrite, covellite, and minor amounts of chalcocite that are cut and surrounded by enargite. An additional reopening of these veins resulted in the deposition of more pyrite, sphalerite with exsolution of tennantite and chalcopyrite, and minor amounts of galena. A final reopening of these late veins formed breccias cemented by alunite that sometimes broke all previous sulfide bands or in some cases only the central part of the vein. Not every vein of the acid-sulfate hydrothermal event includes the complete paragenetic assemblage described above; but they always include pyrite. Beyond the vein walls, fine-grained disseminated pyrite occurs within pervasive acid-sulfate alteration. Where veins of this system cut previous veins, the copper grade is normally from 0.6 to higher than 1 wt percent; pyrite to chalcopyrite ratios are higher than 5:1.

The characteristic overprint of several hypogene mineralizing stages resulted in large volumes of the deposit with 2 vol percent sulfides or more and with hypogene copper grades in excess of 0.5 wt percent. To date no evidence for a potassic core containing high copper grade has been found. In fact, widely spaced deep drilling below high-grade mineralization encountered potassic alteration with sporadic and weak overprinting of later alteration stages (Fig. 10). Copper grades in this deep potassic-altered zone drop to 0.2 wt percent, which is similar to the content of remnants of rock only affected by potassic alteration at high levels in the deposit. Low-fracture intensity (0.2 cm^{-1}) characterizes this deep zone of potassic-altered rock in contrast to the high-fracture intensity (1.0 cm^{-1}) of the upper zone, which is cut by stages 2 and 3. In addition, study of polished sections shows that the content of Cu-Fe sulfides only increases to values higher than 0.5 vol

percent where the chlorite-sericite and green-sericite mineral associations appear on vein halos or when sulfide minerals from the advance argillic event are present in the veins. In contrast, pyrite is the principal sulfide added during the development of the white sericitic event of stage 2.

Crosscutting relationships, sulfide volume percentages, and copper grades from the known part of the hypogene system of the Escondida deposit suggest that hypogene copper grades were upgraded with the development of each hydrothermal stage. Since we have not observed evidence of a potassic core with high copper grade we assume a copper grade of 0.2 wt percent or lower for the whole volume of rock affected for the hydrothermal stage 1. Higher hypogene copper grades (0.6 wt %) occur only where the early orthoclase-biotite–altered rocks are overprinted by fracture-localized mineralization of younger stages. The copper deposited with the chlorite-sericite, quartz-sericite, and advance argillic events could have been the new introduction of metal to the system during the development of these hydrothermal events or, perhaps, was remobilized from the early low-grade K feldspar-quartz ± biotite ± anhydrite assemblage. These two possibilities are real, but we do not have data yet to support or disregard either.

Sulfide enrichment blanket

Supergene ore in the enrichment blanket represents 65 vol percent of the total present copper resources at Escondida. The upper boundary with the oxidized capping is subhorizontal and is offset in several places vertically across fault zones. The lower limit is irregular, resulting in differences in the thickness of this blanket, which varies between a few meters and 400 m (Figs. 10, 11).

Sulfides occur as disseminations and in veins and include fine-grained chalcocite, covellite, and minor amounts of digenite and idaite replacing grains of pyrite, chalcopyrite, and bornite (Alpers and Brimhall, 1989). Chalcocite occurs across the whole thickness of this blanket, but covellite and digenite appear in the middle part and increase in content toward the bottom of this zone (Alpers and Brimhall, 1989). Copper grades typically vary from 0.3 to higher than 2 wt percent but may exceed 3.5 wt percent. The best copper grades occur in the thickest parts of the supergene enrichment blanket, which in turn is associated with the highest intensity of hypogene stockwork. Therefore, the best supergene copper grades overlap the best hypogene copper grades in areas where strong quartz-sericite and advanced argillic events overprint early potassic alteration.

Leached capping zone

The upper limit of the leached capping zone is marked by the modern land surface, whereas its lower limit varies from a few meters below the surface, above the zone of copper oxides, to more than 200 m below the surface, over the enrichment blanket (Figs. 10, 11). Copper and molybdenum grades vary from <100 to 600 ppm and from less than 10 to 480 ppm, respectively (Ortiz et al., 1996). This zone is mainly formed of limonites with compositions that exhibit good spatial correlation with supergene grades and thicknesses (Alpers and Brimhall, 1989). The higher grade and thicker zones of the underlying supergene Cu sulfide blanket are normally below hematite, whereas thinner zones with lower supergene copper grades lie below jarosite-rich capping. Goethite is most abundant in the western part of the deposit where copper oxides are dominant.

Copper oxides

The term "copper oxide" is used to group nonsulfide copper minerals including oxides, silicates, sulfates, and carbonates. This type of mineralization represents 5 vol percent of the total copper resource at Escondida. The most common minerals are brochantite, antlerite, atacamite, chrysocolla, copper wad, and tenorite. They are present mainly along fractures hosted by the andesite with biotite and chlorite-sericite alteration. This ore type is also found in the Escondida stock where K feldspar alteration is preserved, but it is volumetrically less important than in the biotite or chlorite-sericite-altered andesite. In the copper oxide zone, copper grades vary from less than 0.2 to 1.5 wt percent, and the thickness of the mineralized rock ranges from a few meters to 200 m.

Interpretation of the hydrothermal evolution of the Escondida deposit

Alteration mineral stability relationships as a function of cation activity ratios in the hydrothermal fluids at Escondida (cf. Beane, 1982) imply that the early alteration stage, zoned from K silicate to propylitic, was formed under high $a_{(K^+)}/a_{(H^+)}$ and high $a_{(Ca^{++})}/a$ conditions, where $a_{(H^+)}$ represents the thermodynamic activity of H^+ ion in the hydrothermal solution. Under high $a_{(Ca^{++})}/a$ conditions and a high-temperature environment, grossular garnet can form in the propylitic halo (Beane, 1982). In the same alteration zone, the decrease in temperature and in the $a_{(Ca^{++})}/a$ ratio allows the formation of epidote. At Escondida, calcic garnet is present in the propylitic zone, but the most abundant mineral of this alteration zone is epidote. Potassic alteration developed under conditions of a high $a_{(K^+)}/a_{(H^+)}$ ratio, maybe synchronously with the development of garnet in the propylitic zone and under similar conditions of temperature. The potassic alteration in the intrusive rock is mainly represented by addition of K feldspar, whereas in the Mg-rich volcanic rock it is represented by addition of Mg biotite (phlogopite).

A decrease over time of the $a_{(K^+)}/a_{(H^+)}$and $a_{(Ca^{++})}/a$ ratios, via a decrease in pH, resulted in the formation of the younger chlorite-sericite alterations and their associated sulfides. Previous biotite and sometimes K feldspar was altered to chlorite ± sericite and eventually to sericite + quartz. At Escondida, the earliest stage of mineralization associated with potassic alteration is characterized by magnetite, chalcopyrite, and bornite in association with biotite, anhydrite, and K feldspar, suggesting high oxygen fugacity with respect to sulfur fugacity (Beane and Titley, 1981). Sulfides associated with chlorite-sericite and quartz-sericite alterations are chalcopyrite-pyrite with erratic molybdenite, indicating an increase of sulfur fugacity with respect to oxygen fugacity (Beane and Titley, 1981). Sulfide deposition during the second hydrothermal stage was probably triggered by a drop in temperature during the cooling and uplifting of the system. Perhaps sulfide deposition was also enhanced by a decrease in chloride concentration during mixing of nonmagmatic water into the magmatic water and by an increase in pH of the solution due to the

consumption of H^+ during the alteration process (Barnes, 1979).

The latest hydrothermal stage represented by the advanced argillic assemblages is apparently at least 3 m.y. younger than the first two stages associated with the emplacement of the Escondida stock. The source of heat and acidic fluids associated with the formation of the younger advanced argillic alteration-mineralization is subject to debate. Possible explanations could include an independent acid-sulfate event related to emplacement of the rhyolitic domes or acidic fluids that formed by the mix of meteoric water and a magmatic vapor exolved from a younger deep intrusive system emplaced in the same structural zone and maybe associated with the late dikes described above.

Summary and Discussion of Escondida Geology

Structure

At Escondida, the development of the sinistral mineralized north-northwest–striking fault system is interpreted to be synchronous with the emplacement of all the intrusive rocks mapped in the deposit and to the evolution of the hydrothermal system. The second family of faults postdates the emplacement of intrusive rocks and alteration-mineralization. This late fault system shows a dextral sense of displacement along northeast-striking faults (Fig. 7).

A dynamic and kinematic analysis of the mineralized fault system suggests a direction of maximum stress and shortening to be N 39° W, whereas the direction of minimum stress and maximum extension was N 50° E (Figs. 8 and 12). Faults of the mineralized fault system are geometrically consistent with a simple shear model in a transcurrent environment where the north-northwest–striking faults represent the principal deformational zone (PDZ, Fig. 12), whereas the west-northwest–striking faults are interpreted as secondary Reidel (R, R') and tensile (T) structures (Fig. 12). The faults located at angles between 10° and 20° from the principal deformational zone are synthetic Reidel (R) structures. Faults at angles higher than 65° from the principal deformational zone seem to be in antithetic Reidel (R') position; however, their sense of movement is also sinistral, which does not hold with the simple shear model. This kinematic inconsistency may be due to late reactivations associated with the activity of the postmineralization faults. The preferential west-northwest strike of mineralized veins, the Escondida stock, pebble dikes, and late barren dikes are coincident with the position of tensile (T) and Reidel (R, R') structures. In an ideal model, Reidel structures would be closed and only affected by shearing. However, the tendency of Reidel fractures to behave as a combination of shear and extensional fractures could have been facilitated by high pore fluid pressure and by fault rotation.

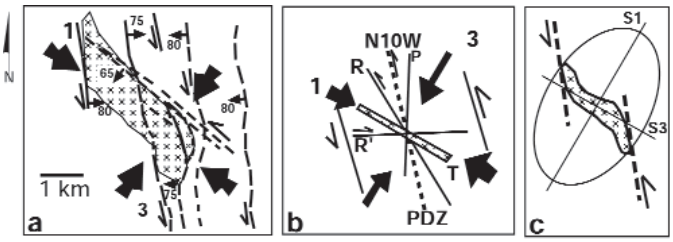

FIG. 12. Structural interpretation of the Escondida deposit. a. Main structural elements and the shape of the Escondida stock at 2,800 m above sea level (patterned area). b. Ideal simple-shear left-lateral strike-slip zone and Riedel shear array (Davis and Reynolds, 1996). R = synthetic, R' = antithetic to main movement on the principal displacement zone (PDZ, dashed line), P = late synthetic shear fractures, T = tensile fractures (squares). c. Plan view projection of strain ellipsoid with the calculated orientations of S_1 and S_3 within a sinistral N 10° W shear zone and the simplified shape of the Escondida stock in plan view.

The model presented in this paper proposes the formation of the Escondida porphyry system during the coeval evolution of a transcurrent fault system and the injection of magmas into a tensional gash. It is proposed that the Escondida stock was emplaced in a large tensional gash developed between the Ferrocarril and the Panadero-Ortiz fault zones (Fig.12). The geometry of faults and the position of the Escondida stock is interpreted as a stepover between these two sinistral strike-slip faults (Fig. 12). In a left-lateral displacement situation, the area of the stepover would have been under extensional conditions (Fig. 12). Therefore, as expected by the Coulomb failure theory (Davis and Reynolds, 1996), a tensile zone formed perpendicular to the least principal stress (σ_3) and later rotated forming a cymoidal final geometry (Fig. 12). It is probable that the main nothwest-striking shear zones (Zaldivar, Panadero, Ortiz, Portezuelo, and Ferrocarril) facilitated the upward movement of a buoyant magma. Once this magma reached the tensile gash, in the upper crust, the magma was initially oriented in a northwest-southeast direction, roughly parallel to the stepover and to the orientation of the maximum principal stress (σ_1) and maximum shortening calculated for the mineralized faults. The magma then expanded in the N 50° E direction parallel to the axis of maximum extension and least principal stress (σ_3). This combination resulted in the N 40° W elongated shape of the Escondida intrusive stock (Fig. 12).

The contacts of the intrusive rock and the andesitic host rock are sharp and xenoliths of andesite are not common within the Escondida stock. This lack of xenoliths may reflect a passive intrusive process, perhaps facilitated by the subhorizontal position of the least principal stress (σ_3) within a strike-slip environment allowing the expansion of magma in the northeast direction. Tensile gashes are observed at small scales associated with strike-slip faults (Woodcock and Schubert, 1994). The large length and width of the tensional gash proposed as a structural host of the Escondida stock were probably enhanced by the injection of magma and aqueous fluids that kept the pore fluid pressure high during the development of the porphyry system, facilitating the formation and growth of tensional structures. The northwest-southeast maximum principal stress orientation was active at least from the earliest stages of veining to the latest stages of postmineral dikes.

Strike-slip structural fault zones are characterized by the presence of compressional and extensional conditions at the same time (Fisher, 1985; Woodcock and Schuber, 1994). This situation generates differential pressure in the upper crust that may facilitate the movement of magmas and aqueous fluids, resulting sometimes in the development of magmatic-hydrothermal systems. Sibson (1987) proposed a mechanism called "fault valve behavior," suggesting that earthquakes

trigger the movement of aqueous fluids to low-pressure areas within fault zones. Other authors have investigated the emplacement of plutons and hydrothermal systems along strike-slip faults (cf. D'Lemos et al., 1992; Monrand, 1992; Paterson and Fowler, 1993). The model proposed in this paper is limited by very little data in the vertical axis. Additional structural studies in the Escondida district and other mining districts located along the Domeyko fault system could help to increase our knowledge in the processes that control the shallow emplacement of hydrous magmas associated with the development of porphyry systems along strike-slip faults.

Ore deposit lithology-alteration-mineralization

Three magmatic intrusive events have been recognized at the Escondida deposit. The first one is the Colorado Grande intrusion with a U-Pb age on zircons of 37.9 ±1.1 Ma reported by Richards et al. (2001). It is possible that the other two quartz-feldspathic porphyritic intrusive phases of the Escondida stock have a similar age. At least 3 m.y. later a rhyolitic dome and a rhyolitic dike were intruded and cut the Escondida porphyritic stock (Alpers and Brimhall, 1988; Zentilli et al., 1994; Richards et al., 1999; Fig. 6). The youngest intrusive event is represented by the intrusion of unmineralized, weakly sericite-altered, narrow quartz-monzonitic dikes that cut the rhyolite (Fig. 6).

Alpers and Brimhall (1988) proposed that the hydrothermal system at Escondida developed between 33.7 ± 1.4 and 31.0 ± 1.4 Ma; however, this age may represent the time of emplacement of the rhyolite and late barren dikes (Richards et al., 2001). Additional U-Pb ages on zircons from different intrusive phases in combination with Re/Os ages from sulfides and Ar^{40}/Ar^{39} ages from K silicate alteration minerals could be used to bracket with more detail the time evolution of the magmatic-hydrothermal system at the Escondida deposit.

The dynamic magmatic-hydrothermal evolution of the Escondida porphyry system is manifested in the alteration-mineralization style of the deposit, characterized by overprinting of veinlet and pervasive events. Three main hydrothermal stages are recognized. The earliest one includes propylitic, silicification, and K feldspar-biotite (potassic) assemblages with magnetite, bornite, and chalcopyrite; the second stage includes chlorite-sericite and quartz-sericite alterations with chalcopyrite, pyrite, and molybdenite. The latest hydrothermal stage is represented by an acid-sulfate alteration with a quartz-pyrophyllite-alunite mineral assemblage. The more than 2 Gt of ore with more than 1 wt percent of copper, reported as reserves of the Escondida deposit, are located where the three main hydrothermal stages are fully overlapped.

The supergene alteration-mineralization is well developed in areas of strong overprinting of the three hydrothermal stages (Figs. 10 and 11). In contrast, in areas with potassic alteration and only a weak development of chlorite-sericite alteration, the supergene process was less effective probably due to the low content of pyrite and by the buffer capacity of biotite and orthoclase (Fig. 11). This is perhaps the reason why the main copper-oxide resource of Escondida is hosted by the biotitic-altered andesite with weak chloritization. The age of formation of the supergene blanket as determined by K-Ar analysis of supergene alunites ranges from 18 to 14.6 Ma (Alpers and Brimhall, 1988). Alpers and Brimhall (1988) also estimated rates of erosion during the formation of the supergene enrichment of 42 m/m.y. as compared to only 9 m/m.y. of denudation from 14 Ma (end of the enrichment) until today.

The overprinting style of the hydrothermal evolution of the Escondida deposit was an important factor in the formation of the copper-rich hypogene ore of the porphyry copper system. However, once the hypogene part of the deposit was formed and exposed to the surface, a low rate of denudation was important in the formation of the supergene enrichment and its preservation. Another important factor in the formation and preservation of the supergene enrichment was the change in climatic conditions (Alpers and Brimhall, 1988). For instance, the formation of the high Andes to the east of Escondida formed a wall that isolated the region from the rain that comes from the Brazilian Shield. Moreover, beginning at about 14 Ma, and extending to the present, the cold waters of the Humboldt current have been migrating from the Antarctic to the northern coast of Chile, where the upwelling of this cold water inhibits evaporation in the west coast of the Atacama region (Alpers and Brimhall, 1988). This has produced the hyperarid conditions of the Atacama dessert, thus preserving the supergene copper mineralization for 14 m.y.

Consequently, the variations in climatic conditions, low rates of denudation during and after the development of the supergene enrichment, the size of the porphyry copper system, and its characteristic alteration-mineralization overprinting were all fundamental factors in the formation and preservation of the rich supergene blanket at Escondida.

Acknowledgments

We are extremely grateful to BHP Minerals and Minera Escondida Ltd. for providing financial support and permission to publish these results. Hugo Dummett, former vicepresident and group general manager of the Discovery group of BHP Minerals, deserves special recognition for initiating and supporting the development of this study. We also acknowledge Manuel Duran, former chief geologist of Escondida, for his important initial support of this study. The geological and technical staff of Minera Escondida provided excellent support, particularly, Nicolas Cruz, Carlos Alcayaga, Jonathan Gilligan, Guillermo Segovia, and Luis Luengo. Jim Bratt of BHP Minerals, Hector Veliz, Eduardo Medina, and Hans Niemeyer of the Universidad del Norte deserve special credit for their contributions during the period when much of the fieldwork was done. The manuscript benefited from the comments of Joaquin Ruiz, Mark Barton, Pepe Perelló, and Lukas Zurcher and by detail reviews from John Dilles, Charles Alpers, and Darryl Lindsay.

REFERENCES

Allmendinger, R.W., Gephart, J.W., and Marrett, R.A., 1989, Notes on fault slip analysis: Geological Society of America Short Course on "Quantitative Interpretation of Joints and Faults, p. 1–56.

Allmendinger, R.W, Marrret, R.A., and Claudouhos, T., 1993, Fault kinematics v.3.5a: A software for determination of finite strain and rotation from fault-slip data: Journal of Structural Geology, v. 12, p. 771–784.

Alpers, C.N., 1986, Geochemical and geomorphological dynamics of supergene copper sulfide ore formation and preservation at La Escondida, Antofagasta, Chile: Unpublished Ph.D. thesis, Berkeley, California, University of California, 184 p.

Alpers, C.N., and Brimhall, G.H, 1988, Middle Miocene climatic changes in the Atacama Desert, northern Chile: Evidence from supergene mineralization at La Escondida: Geological Society of America Bulletin, v. 100, p. 1640–1656.
——1989, Paleohydrologic evolution and geochemical dynamics of cumulative supergene metal enrichment at La Escondida, Atacama Desert, northern Chile: Economic Geology, v. 84, p. 229–255.
Ardill, J., Flint, S., Chong, G., and Wilke, H., 1998, Sequence stratigraphic of the Mesozoic Domeyko basin, northern Chile: Journal of the Geological Society of London, v. 155, p. 71–88.
Bahlgurg, H., and Herve, F., 1997, Geodynamic evolution and tectonostratigraphic terranes of NW-Argentina and northern Chile: Geological Society of America Bulletin, v. 109, p. 889–894.
Baker, R.C., and Guilbert, J.M., 1987, Regional structural control of porphyry copper deposits in northern Chile [abs.]: Geological Society of America Abstract with Programs, p. 578.
Barnes, H.L., 1979, Solubilities of ore minerals, *in* Barnes, H.L., ed., Geochemistry of hydrothermal ore deposits, 2nd ed.: New York, J. Wiley and Sons, p. 404–454.
Beane, S.R., 1982, Hydrothermal alteration in silicate rock, *in* Titley, S.R., ed., Advances in geology of the porphyry copper deposits, southwestern North America: Tucson, University of Arizona Press, p. 117–127.
Beane, S.R., and Titley, R.E., 1981, Porphyry copper deposits. Part II. Hydrothermal alteration and mineralization: Economic Geology 75th Anniversary Volume, p. 235–269.
Boric, R.P., Diaz, F.F., Maksaev J., V., 1990, Geología y yacimientos metalíferos de la region de Antofagasta: Sevicio Nacional de Geología y Mineria de Chile, Bull. 40, p. 246.
Coney, P.J., and Evenchick, C.A., 1994, Consolidation of the American cordilleras: Journal of South American Earth Science, v. 7, p. 241–262.
Cornejo, P.P., and Mpodozis, C., 1996, Geologia de la Region de Sierra Exploradora: Servicio Nacional de Geologia y Mineria Boletin IR-96-09, v. 1, p. 250–350.
Davis, H.G., and Reynolds, J.S., 1996, Structural geology, 2nd ed.: New York, J. Wiley and Sons, 775 p.
Dilles, J.H., Martin, M.W., Tomlinson, M.W., and Blanco, N., 1997, El Abra and Fortuna complexes: A porphyry copper batholit sinistral displaced by the Falla Oeste: Congreso Geológico Chileno, 8th, Antofagasta, Chile, Universidad Católica del Norte, v. 3, p. 1873–1883.
D'Lemos, R.S., Brown, M., and Strachan, R.A., 1992, Granite magma generation, ascent, and emplacement within a transpressional orogen: Journal of the Geological Society of London, v. 149, p. 487–498.
Fischer, M., 1985, Strike-slip faults: Journal of Structural Geology, v. 8, p. 725–740.
Gustafson, L.B., and Hunt J.P., 1975, The porphyry copper deposit at El Salvador, Chile: Economic Geology, v. 70, p. 857–912.
Hardcastle, K.C., and Hills, L.S., 1991, Brute 3: Quickbasic 4 programs for determination of stress tensor configurations and separation of heterogeneous populations of fault-slip data: Computers and Geosciences, v. 17, p. 23–43.
Lindsay, D.D., Zentilli, M., and Rojas de la Rivera, J., 1995, Evolution of an active ductile to brittle shear system controlling mineralization at the Chuquicamata porphyry copper deposit, northern Chile: International Geology Review, v. 37, p. 945–958.
Marinovic, N., Smoje, I., Masksaev, V., Herve, M., and Mpodozis, C., 1992, Hoja de Aguas Blancas, Region de Antofagasta: Servicio Nacional de Geologia y Mineria, Carta geologica de Chile 70, scale, 1: 250,000.
McKinstry, H.E., 1948, Mining geology: Englewood Cliffs, New Jersey, Prentice-Hall, 680 p.
Monrand, V.J., 1992, Pluton emplacement in a strike-slip fault zone: The Doctors flat pluton, Victoria, Australia: Journal of Structural Geology, v. 14, p. 205–214.
Mpodozis, C., and Ramos, V.A., 1990, The Andes of Chile and Argentina: Circum Pacific Council for Energy and Mineral resources, Earth Sciences Series, v. 11, p. 59–90.
Mpodozis, C., Marinovic, C., and Smoje, I., 1993, Eocene left lateral strike-slip faulting and clockwise rotations in the Cordillera de Domeyko, west of Salar de Atacama, northern Chile: International Symposium on Andean Geodynamics, 2nd, p. 195–198.
Ojeda, J.M., 1986, Escondida porphyry copper deposit, II region, Chile: Exploration, drilling and interpretation: Mining Latin America Conference, Institute of Mining and Metallurgy, p. 299–318.
——1990, Geology of the Escondida porphyry copper deposit, II region, Chile: Pacific Rim Congress, 90th, Australian Institute of Mining and Metallurgy, Canberra, Proceedings, p. 473–483.
Ortiz, F.J., Lowell, J.D., Bratt, J.A., Rojas, N.D., and Burns, P.J., 1996, Escondida porphyry copper deposit, II region, Chile: History of the discovery: Mining Latin America Conference, Institute of Mining and Metallurgy, Santiago, Chile, Proceedings, p. 319–331.
Paterson, S., and Fowler, T.K., Jr., 1993, Re-examining pluton emplacement processes: Journal of Structural Geology, v. 15, p. 191–206.
Pardo-Casas, F., and Molnar, P., 1987, Relative motion of the Nazca and South American plates since Late Cretaceous time: Tectonics, v. 6, p. 233–248.
Perelló, J., 1983, Al menos tres etapas en la evolucion del "Porfido Principal" de Escondida: Nota de trabajo, Antofagasta, Chile: Minera Utah de Chile, Inc., internal memorandum, 6 p.
——1984, Geological setting of the Escondida porphyry copper deposit, Antofagasta, Chile: Minera Utah de Chile, Inc., internal memorandum, 11 p.
Petit, J., 1987, Criterions of sense movement in brittle rock: Journal of Structural Geology, v. 9, p. 238–256.
Prinz, P., Hans, G.W., and Hillerbrandt, A.V., 1994, Sediment accumulation and subsidence history in the Mesozoic marginal basin of northern Chile, *in* Reutter, K.L., Scheuber, E., and Wigger, P.J., eds., Tectonics of the southern Central Andes: Berlin, Springer-Verlag, p. 219–248.
Quiroz, F.L., 1998, Reporte sobre la geologia del porfido cuprifero Escondida, Antofagasta, Chile: Antofagasta, Chile, Minera Escondida Ltd., internal report, 50 p.
Ramos, V.A., 1988, The birth of southern South America: American Scientist, v. 77, p. 444–450.
Reutter, K.L., and Sheuber, E., 1991, Structural evidence of orogen-parallel strike-slip displacements in the Precordillera of northern Chile: Geologische Rundschau, v. 80, p. 125–153.
Richards, J.P., Noble, S.R., and Pringle, M.S., 1999, A revised late Eocene age for porphyry Cu-forming magmatism in the Escondida area, northern Chile: Economic Geology, v. 94, p. 1231–1247.
Richards, J.P., Boyce, A.J., and Pringle, M., 2001, Geologic evolution of the Escondida area, northern Chile: A model for spatial and temporal localization of porphyry Cu mineralization: Economic Geology, v. 96, p. 271–305.
Scheuber, E., and Reutter, K., 1992, Magmatic arc tectonics in the Central Andes between 21° and 25° latitude South, Andean geodynamics: Tectonophysics, v. 205, p. 127–140.
Sibson, R.H., 1987, Earthquake rupturing as mineralizing agent in hydrothermal systems: Geology, v. 15, p. 701–704.
Sillitoe, R.H., 1981, Regional aspects of the Andean porphyry copper belt in Chile and Argentina: Institution of Minining and Metallurgy Transactions, sec. B, v. 90, p. 15–16.
——1988, Epochs of intrusion-related copper mineralization in the Andes: Journal of South American Earth Sciences, v. 1, p. 89–108.
Sillitoe, R.H., and McKee, E.H., 1996, Age of supergene oxidation and enrichment in the Chilean porphyry copper province: Economic Geology, v. 91, p. 164–179.
Titley, S.R., and Heidrick, T.L., 1978, Intrusion and fracture styles of some mineralized porphyry systems of the southwestern Pacific and their relationship to plate interaction: Economic Geology, v. 73, p. 891–903.
Tomlinson, M.W., and Blanco, N., 1997a, Structural evolution and displacement history of the West fault system, pre-Cordillera, Chile: Part I. Synmineral history: Congreso Geológico Chileno, 8th, Antofagasta, Chile, Universidad Católica del Norte, v. 3, p. 1873–1883.
——1997b, Structural evolution and displacement history of the West fault system, pre-Cordillera, Chile: Part II. Postmineral history: Congreso Geológico Chileno, 8th, Antofagasta, Chile, Universidad Católica del Norte, v. 3, p. 1873–1883.
Veliz, H., and Padilla, R.A., 1997, Geologia estructural del yacimiento Escondida: Antofagasta, Chile, Minera Escondida Ltd., internal report, 50 p.
Wilkes, E., and Görler, K., 1994, Sedimentary and structural evolution of the salar de Atacama depression, *in* Reutter, K.L., Scheuber, E., and Wigger, P.J., eds., Tectonics of the southern Central Andes: Berlin, Springer-Verlag, p. 171–187.
Woodcock, N.H., 1987, Strike-slip duplexes: Journal of Structural Geology, v. 8, p. 725–735.
Woodcock, N.H., and Schubert, C., 1994, Continental strike-slip tectonics, *in* Hancock, P.L., ed., Continental Deformation: Oxford, Pergamon Press, p. 121–142.
Zentilli, M., Krogh, T.E., Maksaev, V., and Alpers, C.N., 1994, Uranium-lead dating of zircons from the Chuquicamata and La Escondida porphyry copper deposits, Chile: Inherited zircon cores of Paleozoic age with Tertiary overgrowths: Comunicaciones, no. 45, p. 101–110.